EUKARYOTIC CELL, May 2011, p. 629–645 Vol. 10, No. 5
1535-9778/11/$12.00 doi:10.1128/EC.00015-11

Grx4 Monothiol Glutaredoxin Is Required for Iron Limitation-Dependent Inhibition of Fep1[▽]

Mehdi Jbel, Alexandre Mercier, and Simon Labbé*

Département de Biochimie, Faculté de Médecine et des Sciences de la Santé, Université de Sherbrooke, Sherbrooke, Quebec J1H 5N4, Canada

Received 28 January 2011/Accepted 7 March 2011

The expression of iron transport genes in *Schizosaccharomyces pombe* is controlled by the Fep1 transcription factor. When iron levels exceed those needed by the cells, Fep1 represses iron transport genes. In contrast, Fep1 is unable to bind chromatin under low-iron conditions, and that results in activation of genes involved in iron acquisition. Studies of fungi have revealed that monothiol glutaredoxins are required to inhibit iron-dependent transcription factors in response to high levels of iron. Here, we show that the monothiol glutaredoxin Grx4 plays an important role in the negative regulation of Fep1 activity in response to iron deficiency. Deletion of the *grx4*$^+$ gene led to constitutive promoter occupancy by Fep1 and caused an invariable repression of iron transport genes. We found that Grx4 and Fep1 physically interact with each other. Grx4 contains an N-terminal thioredoxin (TRX)-like domain and a C-terminal glutaredoxin (GRX)-like domain. Deletion mapping analysis revealed that the TRX domain interacts strongly and constitutively with the C-terminal region of Fep1. As opposed to the TRX domain, the GRX domain associates weakly and in an iron-dependent manner with the N-terminal region of Fep1. Further analysis showed that Cys35 of Grx4 is required for the interaction between the Fep1 C terminus and the TRX domain, whereas Grx4 Cys172 is necessary for the association between the Fep1 N terminus and the GRX domain. Our results describe the first example of a monothiol glutaredoxin that acts as an inhibitory partner for an iron-regulated transcription factor under conditions of low iron levels.

Redox-active transition metals such as iron present a dilemma to cells. They are cofactors essential for cell survival but can also be cytotoxic under certain conditions (10, 15). Iron is a micronutrient that serves as a catalytic and a structural cofactor for many enzymes intimately linked to essential cellular functions. Examples include DNA synthesis, the energy-generating respiratory chain, and lipid metabolism, all of which require iron (44). On the other hand, due to its proclivity to undergo changes in redox status within the cell, ferrous iron [Fe^{2+}] can react with hydrogen peroxide to produce the highly toxic hydroxyl radical (9). Consequently, in order to keep adequate, but not excessive, iron levels, organisms have developed regulated mechanisms for acquiring sufficient iron while at the same time preventing the buildup of concentrations that could lead to cell death.

In the model organism *Schizosaccharomyces pombe*, Fep1 and Php4 act as key regulators of iron homeostasis by controlling iron acquisition and iron utilization, respectively (21, 27, 34). In response to elevated concentrations of iron, the GATA-type transcription factor Fep1 represses the expression of several genes, including those encoding components of the reductive (e.g., *frp1*$^+$, *fio1*$^+$, and *fip1*$^+$), nonreductive (e.g., *str1*$^+$, *str2*$^+$, and *str3*$^+$), and vacuolar (*abc3*$^+$) iron transport systems (34–37). Another member of the Fep1 regulon is *php4*$^+$ (27). When the availability of iron is limited, Fep1 fails to act as a repressor resulting in *php4*$^+$ transcription. The CCAAT-binding subunit Php4 coordinates the iron-sparing response by downregulating the genes that encode the components of iron-requiring metabolic pathways such as the tricarboxylic acid (TCA) cycle, the electron transport chain, and the iron-sulfur cluster biogenesis machinery (28). Php4 associates with its target genes by recognition of the CCAAT-binding complex, which is composed of Php2, Php3, and Php5 (25, 27). The Php2/Php3/Php5 heterotrimer binds CCAAT *cis*-acting elements, whereas Php4 lacks DNA-binding activity. Php4 is responsible for the capability of the Php complex to repress transcription in response to iron starvation. It has been demonstrated that the gene encoding the transcriptional repressor Fep1 is regulated by Php4, creating a reciprocal regulatory loop between both iron-responsive sensors (28).

Using a chromatin immunoprecipitation (ChIP) technique and a functional *TAP-fep1*$^+$ (where TAP is a tandem affinity purification tag) fusion allele, we demonstrated that TAP-Fep1 strongly associates with iron-responsive and GATA-containing promoters in iron-replete cells *in vivo*. In contrast, we found that conditions of iron starvation inhibit the binding of TAP-Fep1 to chromatin (14). Deletion mapping analysis revealed that the N-terminal 241-residue segment of Fep1 is necessary and sufficient for maximal iron-dependent binding to chromatin (14). The N-terminal 241-amino-acid region of Fep1 contains two Cys_2/Cys_2-type zinc finger motifs, denoted ZF1 and ZF2. In addition, there is also a conserved 27-residue segment containing four invariant Cys residues that is positioned between the two zinc finger motifs (36). Mutation of two of the conserved Cys residues to Ala resulted in the inability of Fep1 to bind to chromatin, irrespective of the cellular iron status (14). Further analysis by ChIP showed that the region encompassing the Cys-rich domain and ZF2 constitutes the minimal

* Corresponding author. Mailing address: Département de Biochimie, Faculté de Médecine et des Sciences de la Santé, Université de Sherbrooke, 3001, 12[e] Avenue Nord, Sherbrooke, Quebec, Canada J1H 5N4. Phone: (819) 820-6868, ext. 15460. Fax: (819) 564-5340. E-mail: Simon.Labbe@USherbrooke.ca.

[▽] Published ahead of print on 18 March 2011.

module required for the iron-dependent binding of Fep1 to chromatin, whereas the truncation of ZF1 led to a decrease in its binding ability (14). In *Histoplasma capsulatum*, an Fep1-like repressor (denoted Sre1) has been shown to directly bind ferric iron (2). Thus, a current working model for repression by the GATA-type regulators with similar functions and sequences to Fep1 posits that, when bound by iron, the iron-responsive repressors bind to their target GATA sequences within the promoters of the target genes to downregulate transcription. In contrast, when intracellular iron is limited, Fep1 orthologs dissociate from the chromatin, thus allowing the transcription of the target gene. Although these sequences of events are still under investigation, less attention has been paid to the characterization of the mechanism by which Fep1 and its orthologs are inactivated under conditions of iron deprivation.

Studies of *Saccharomyces cerevisiae* have provided additional clues with respect to iron sensing (4, 20, 31, 32, 38, 42). *S. cerevisiae* genes encoding proteins that function in high-affinity iron transport are regulated by Aft1. When iron is scarce, Aft1 accumulates in the nucleus, where it binds to DNA and activates transcription (45, 46, 50). Although the mechanism by which Aft1 is activated remains unclear, it has been shown that the iron-dependent inhibition of Aft1 requires the production of mitochondrial Fe-S clusters (4, 42). That said, the mechanism by which mitochondrial Fe-S cluster synthesis negatively affects Aft1 activity remains unclear. Subsequent studies have shown that the *S. cerevisiae* monothiol glutaredoxins Grx3 and Grx4 are key regulators of Aft1 (32, 38). When cells undergo a transition from iron-limiting to iron-sufficient conditions, it has been proposed that Grx3 and Grx4, with the aid of Fra2 and possibly Fra1, transmit an as-yet-unidentified mitochondrial inhibitory signal which leads to Aft1 inactivation and its subsequent export from the nucleus to the cytoplasm (20, 23, 24). Similarly to Aft1, *S. pombe* Php4 is active during iron deficiency, except that it represses rather than activates transcription. Recently, studies revealed that in cells undergoing a shift from low to high iron concentrations, nuclear inactivation and nuclear exclusion of Php4 require a functional *grx4*$^+$ gene (26).

S. pombe contains two dithiol glutaredoxins (Grx1 and Grx2) with antioxidant functions (5). Grx1 localizes primarily throughout the cytosol, whereas Grx2 is located in the mitochondrion (5). Similarly to other family members of dithiol glutaredoxins, Grx1 and Grx2 are small proteins with thiol oxidoreductase activity. Their active sites are highly conserved and contain two essential Cys residues. In addition, *S. pombe* possesses three monothiol glutaredoxins, denoted Grx3, Grx4, and Grx5, which are found mainly at the nuclear rim, throughout the whole cell (cytosol and nucleus), and in the mitochondria, respectively (6, 26). All three monothiol glutaredoxins contain one highly conserved Cys residue located at the active site, which is included in the glutaredoxin (GRX)-like domain. Interestingly, the Grx4 protein harbors an extra domain at the N terminus that contains a WAAPCK sequence, reminiscent of a thioredoxin active site, which is composed of the WCGPCK motif (6, 11). The N-terminal thioredoxin (TRX)-like domain is also found in the *S. cerevisiae* Grx3 and Grx4 monothiol glutaredoxins (11). This domain has been suggested to be important for the nuclear localization of TRX-containing monothiol glutaredoxins (30). The *S. pombe* Grx4 protein has been proposed to be implicated in nitrosative, osmotic, oxidative, and iron-dependent stress responses (6, 17, 26).

Because several studies pointed to important roles for cytosolic/nuclear monothiol glutaredoxins in the regulation of cellular iron homeostasis (23, 24, 26, 31, 32, 38, 40, 41), the possibility that *S. pombe* Grx4 affects Fep1 activity as a function of iron availability was examined. Initially, mutant strains were created that unlinked the iron-dependent behavior of Fep1 protein from its transcriptional regulation by Php4. In this context, the disruption of the *grx4*$^+$ gene made Fep1 constitutively active and always bound to its target gene promoters *in vivo*. When coexpressed in fission yeast, the Grx4 and Fep1 proteins were detected in a heteroprotein complex by coimmunoprecipitation experiments. Using a two-hybrid analysis, we demonstrated that the TRX domain in Grx4 is necessary for its interaction with the C-terminal region of Fep1. This interaction, which was strong and not modulated by iron, required the minimal module encompassing amino acid residues 405 to 501 of Fep1. Further analysis showed that Cys 35 of Grx4 is necessary for the Fep1-TRX domain interaction. Surprisingly, we found that the GRX domain of Grx4 associates weakly with the N-terminal region of Fep1 in an iron-dependent manner. Site-directed mutagenesis identified Cys 172 of Grx4 as being required for this iron-dependent association. Collectively, the findings reported here provide convincing evidence that Grx4 is a binding partner of Fep1 and that it plays a critical role in inhibiting Fep1 function under conditions of iron deficiency.

MATERIALS AND METHODS

Yeast strains and growth conditions. The genotypes of the *S. pombe* strains used in this study were as follows: FY435 (*h*$^+$ *his7-366 leu1-32 ura4-Δ18 ade6-M210*), *php4Δ* (*h*$^+$ *his7-366 leu1-32 ura4-Δ18 ade6-M210 php4Δ::KAN*^{r}), *fep1Δ* (*h*$^+$ *his7-366 leu1-32 ura4-Δ18 ade6-M210 fep1Δ::ura4*$^+$), *grx4Δ* (*h*$^+$ *his7-366 leu1-32 ura4-Δ18 ade6-M210 grx4Δ::KAN*^{r}), *fep1Δ php4Δ* (*h*$^+$ *his7-366 leu1-32 ura4-Δ18 ade6-M210 fep1Δ::KAN*^{r} *php4Δ::loxP*), *php4Δ grx4Δ* (*h*$^+$ *his7-366 leu1-32 ura4-Δ18 ade6-M210 php4Δ::loxP grx4Δ::KAN*^{r}) and *fep1Δ php4Δ grx4Δ* (*h*$^+$ *his7-366 leu1-32 ura4-Δ18 ade6-M210 php4Δ::loxP fep1Δ::loxP grx4Δ::KAN*^{r}). All seven strains were cultured in yeast extract supplemented (YES) medium containing 0.5% yeast extract and 3% glucose that was supplemented with 225 mg/liter of adenine, histidine, leucine, uracil, and lysine, unless otherwise stated. Strains for which plasmid integration was required were grown in synthetic Edinburgh minimal medium (EMM) lacking the specific nutrients required for plasmid selection and maintenance. Cells were seeded at an A_{600} of 0.5, grown to exponential phase (A_{600} of ~1.0), and then either cultured in the presence of 2, 2′-dipyridyl (Dip) (250 μM) or $FeCl_3$ (100 or 250 μM) or left untreated for 90 min, unless otherwise indicated. *S. pombe grx4Δ*, *php4Δ grx4Δ*, and *fep1Δ php4Δ grx4Δ* disruption strains, as well as control strains, were grown in culture jars under microaerobic conditions using a BD GazPack EZ system (BD Diagnostic System, Sparks, MD). In the case of two-hybrid experiments, *S. cerevisiae* strain L40 [*MAT***a** *his3Δ200 trp1-901 leu2-3,112 ade2 LYS2*::(*lexAop*)$_4$*-HIS3 URA3*::(*lexAop*)$_8$*-lacZ*] (47) was grown in a synthetic minimal medium containing 83 mg/liter of histidine, adenine, uracil, and lysine plus 2% dextrose, 50 mM MES [2-(*N*-morpholino)ethanesulfonic acid] buffer (pH 6.1), and 0.67% yeast nitrogen base lacking copper and iron (MP Biomedicals, Solon, OH).

Plasmids. The pJK-1478NTAP*fep1*$^+$ plasmid has been described previously (36). To create the pBPade6-1478*fep1*$^+$*-RFP* plasmid, pJK-1478*fep1*$^+$*-GFP* (where GFP is green fluorescent protein) was codigested with SacII and SalI, thereby allowing the purification of a DNA fragment containing the *fep1*$^+$ gene along with its promoter. The purified DNA fragment was cloned into SacII-SalI-digested pBP*ade6*$^+$ vector (1). The SalI and Asp718 restriction sites were used to insert, in frame, a copy of the red fluorescent protein (RFP) gene (kind gift of Richard Rachubinski, University of Alberta, Canada). The pJK-1200*grx4*$^+$ plasmid was constructed via a three-piece ligation protocol by simultaneously introducing the SacII-BamHI *grx4*$^+$ promoter fragment and the BamHI-SalI *grx4*$^+$ gene fragment into the SacII-SalI-digested pJK210 vector (16). The *GFP* coding sequence with SalI and Asp718 sites at the 5′ and 3′ termini, respectively, of the *GFP* gene was derived from pSF-GP1 (18) by PCR. The resulting DNA fragment

was used to clone the *GFP* gene into the pJK-1200*grx4*$^+$ plasmid to which SalI and Asp718 restriction sites, placed immediately before the *grx4*$^+$ stop codon, had previously been introduced by PCR. For this particular construct, the SalI-Asp718 *GFP*-encoded fragment was placed in frame with the C-terminal region of Grx4. A copy of the *TAP* coding sequence was generated by PCR from the pEA500-194prom*php4*$^+$-*TAP* plasmid (26) using primers that contained BamHI and Asp718 sites and then was exchanged with the BamHI-Asp718 DNA fragment in plasmid pJK-1478*fep1*$^+$ (36). The resulting recombinant vector expressed the TAP alone under the control of the *fep1*$^+$ promoter.

For two-hybrid interaction assays, either the complete or the truncated versions of the *fep1*$^+$ gene were generated by PCR using primers that contained BamHI and NotI restriction sites. Subsequently, the purified DNA fragments were digested with these enzymes and cloned into the corresponding sites of pVP16 (47) as described previously (51). To clone the *grx4*$^+$ gene and its mutant derivatives into the pLexN-a vector (47), primers designed to generate BamHI and SalI restriction sites at the upstream and downstream termini of the coding sequences were used. The *grx4* mutant alleles containing either site-specific mutations (e.g., *C35A* or *C172A*) or N- or C-terminal deletions (e.g., *grx4*Δ*TRX* or *grx4*Δ*GRX*) were created by the overlap-extension method (12). The final PCR products were digested with BamHI and SalI and then were cloned into the corresponding sites of pLexN-a. The LexA-Tup11 and VP16-Fep1 fusion proteins served as controls for the two-hybrid analysis (51).

Analysis of gene expression. Total RNA was extracted using a hot phenol method as described previously (3). RNA samples were quantified spectrophotometrically, and 15 μg of RNA per sample was used for RNase protection assays, which were carried out as described previously (28). The riboprobes derived from the plasmids pSK*fep1*$^+$ (14), pSK*fio1*$^+$ (34), and pSK*act1*$^+$ (27) were used to detect *fep1*$^+$, *fio1*$^+$, and *act1*$^+$ transcripts, respectively. The *act1*$^+$ riboprobe was used to detect *act1*$^+$ mRNA as an internal control for normalization during quantification of the RNase protection products. The riboprobes derived from the plasmids pKS*ACT1* (22) and pSK*VP16* (26) were used to determine the *ACT1* (from *S. cerevisiae*) and *VP16* mRNA levels, respectively.

Chromatin immunoprecipitation. The preparation of chromatin was carried out as described previously (14). Immunoprecipitation of TAP-tagged Fep1 with immunoglobulin G (IgG)-Sepharose beads and the subsequent elution of the immunocomplexes were performed as described previously (14). To reverse the formaldehyde cross-links, both the eluted DNA and the DNA of the input control were first incubated at 65°C for 18 h and then at 37°C for 2 h in the presence of 50 μg of proteinase K. Free DNA was then purified as described previously prior to PCR analysis (14). PCR amplifications were performed essentially as described by Komarnitsky et al. (19), except that the PCR program consisted of 2 min at 94°C, followed by 25 cycles of 1 min at 94°C, 1 min at 55°C, and 2 min at 72°C, with a final 4-min step at 72°C. Radiolabeled PCR products were purified using Quick Spin columns (Roche Diagnostics, Indianapolis, IN) and were resolved in 6% polyacrylamide–1× Tris-borate-EDTA gels. PCR signals were quantified by PhosphorImager scanning and were then normalized with respect to both the input DNA reaction mixture and the internal intergenic control primer pair (in order to correct for PCR efficiency and background signals). All experiments were performed at least three times, and each experiment yielded similar results. Primers that span the *fio1*$^+$ promoter region that included functional GATA boxes (34) were used for PCR analysis. The primers were designated by the name of the gene promoter, followed by the position of their 5′ ends relative to the translational initiation codon: fio1-a$_{-884}$, 5′-CACCGCGTTAG GGCAAACAGGCCGGGGGGAAGCATGCCC-3′; fio1-b$_{-724}$, 5′-GATAGGAC AGTTTTGGGGTCGGAGTTGGTGTCCACTTTG-3′; Intergenic-cII3860000-a, 5′-CGGTGCGTTTTTCTACGCGCATCTTC-3′; Intergenic-cII3860000-b, 5′-GC CCAAGGCCCATCAACAATCTAACATG-3′.

Fluorescence microscopy. Fluorescence microscopic analysis was performed as described previously (14). Fluorescence and differential interference contrast images of the cells were obtained using an Eclipse E800 epifluorescent microscope (Nikon, Melville, NY) equipped with an ORCA ER digital cooled camera (Hamamatsu, Bridgewater, NJ). The samples were analyzed using a magnification of ×1,000 with the following filters: 465 to 495 nm (GFP) and 510 to 560 nm (RFP). Cell fields shown in this study are representative of a minimum of five independent experiments. The merged images were obtained using the Simple PCI software, version 5.3.0.1102 (Compix, Sewickly, PA).

Coimmunoprecipitation. To determine whether Grx4 interacted with Fep1 in *S. pombe*, *fep1*Δ *php4*Δ *grx4*Δ cells were cotransformed with either pJK-1200*grx4*$^+$-*GFP* or its mutant derivatives and pJK-1478NTAP-*fep1*$^+$. As a control for signal specificity, cells were also cotransformed with pJK-1200*grx4*$^+$-*GFP* and pJK-1478NTAP. The cells were grown to an A_{600} of 0.9 and were then incubated in the presence of 250 μM Dip or 100 μM $FeCl_3$ for 90 min. Total cell lysates were obtained by glass bead disruption in lysis buffer (10 mM Tris-HCl [pH 7.9], 0.1% Triton X-100, 0.5 mM EDTA, 20% glycerol, 100 mM NaCl, and 1 mM phenylmethylsulfonyl fluoride) containing a mixture of protease inhibitors (P-8340; Sigma-Aldrich). After centrifugation at 13,000 rpm at 4°C for 5 min, equal amounts of proteins (~5 mg) were added to 15-μl bed volumes of IgG-Sepharose 6 Fast-Flow beads (GE Healthcare) and the mixtures tumbled for 4 h at 4°C. The beads were washed four times with 1 ml of lysis buffer and then were transferred to a fresh microtube prior to a final wash. The immunoprecipitates were resuspended in 60 μl of SDS loading buffer and heated for 5 min at 95°C, and the proteins were resolved by electrophoresis on a 9% SDS-polyacrylamide gel. For Western blotting of TAP-Fep1, Grx4-GFP, and PCNA, the following primary antisera were used: polyclonal anti-mouse IgG antibody (ICN Biomedicals, Aurora, OH), monoclonal anti-GFP antibody B-2 (Santa Cruz Biotechnology, Santa Cruz, CA), and monoclonal anti-PCNA antibody PC10 (Sigma-Aldrich).

Two-hybrid analysis. Precultures of each L40 cotransformed strain harboring the indicated bait and prey plasmids were grown to an A_{600} of 0.3 and were then either left untreated or cultured in the presence of Dip (250 μM) or $FeCl_3$ (100 μM) for 4 h. Aliquots were withdrawn, and β-galactosidase activity was assayed using *o*-nitrophenyl-β-D-galactopyranoside as a substrate (51). The β-galactosidase activity levels were measured within the linear response range, and values are expressed in standard units (29). The values reported here are the averages of triplicate assays of three independent cotransformants. The antibodies used for protein expression analysis were the monoclonal antibodies anti-LexA 2-12, which is directed against the LexA DNA binding domain, and anti-VP16 1-21, which is directed against the VP16 activation domain (Santa Cruz Biotechnology, Santa Cruz, CA). A monoclonal anti-3-phosphoglycerate kinase (PGK) antibody (Molecular Probes, Eugene, OR) was used to detect PGK that served as an internal control.

RESULTS

Fep1 is inhibited by a Php4-independent mechanism. When *S. pombe* cells are grown under low iron conditions, the CCAAT-binding factor Php4 is synthesized and interacts with the Php2/Php3/Php5 heterotrimer to mediate repression of the *fep1*$^+$ gene (28). Surprisingly, we have observed that even in the absence of Php4 (*php4*Δ mutant), Fep1 was inactivated under conditions of iron deficiency. In these circumstances, its target genes (e.g., *fio1*$^+$) were clearly upregulated in response to iron starvation (Fig. 1A and B; also data not shown). This Php4-independent mechanism was not active at the transcriptional level because the *fep1*$^+$ mRNA levels were constitutive and were unaffected by iron deprivation (Fig. 1C and D). To gain further insight into the mechanism of the Php4-independent inactivation of Fep1 under conditions of iron starvation, we created a series of mutants in which several putative homeostasis genes were disrupted in combination with the *php4*$^+$ gene. Using these mutant strains, we discovered that a *php4*Δ strain in which the *grx4*$^+$ gene was insertionally inactivated (*php4*Δ *grx4*Δ) exhibited very low *fio1*$^+$ mRNA levels, even in the presence of the iron chelator Dip (Fig. 1A and B). As a control, wild-type cells (FY435) displayed *fio1*$^+$ transcript levels that were repressed only in the presence of basal and high iron concentrations, whereas *fio1*$^+$ mRNAs were induced exclusively in response to iron starvation (Fig. 1A and B). Importantly, the negative effect of the deletion of Grx4 on *fio1*$^+$ expression was corrected by inactivating the *fep1*$^+$ allele (*php4*Δ *grx4*Δ *fep1*Δ), revealing that the repression observed in *php4*Δ *grx4*Δ mutant cells required a functional Fep1 protein (Fig. 1A and B). As previously shown in the case of the *fep1*Δ single mutant (14, 34, 36), *php4*Δ cells harboring an inactivated *fep1*$^+$ gene (*php4*Δ *fep1*Δ) exhibited a strong constitutive transcription of *fio1*$^+$ regardless of the iron status (Fig. 1A and B). Concomitantly, the *fep1*$^+$ transcript levels were validated. *fep1*$^+$ mRNA was detected in strains expressing *fep1*$^+$, whereas it was absent in *fep1*Δ mutant cells. As a control for normal

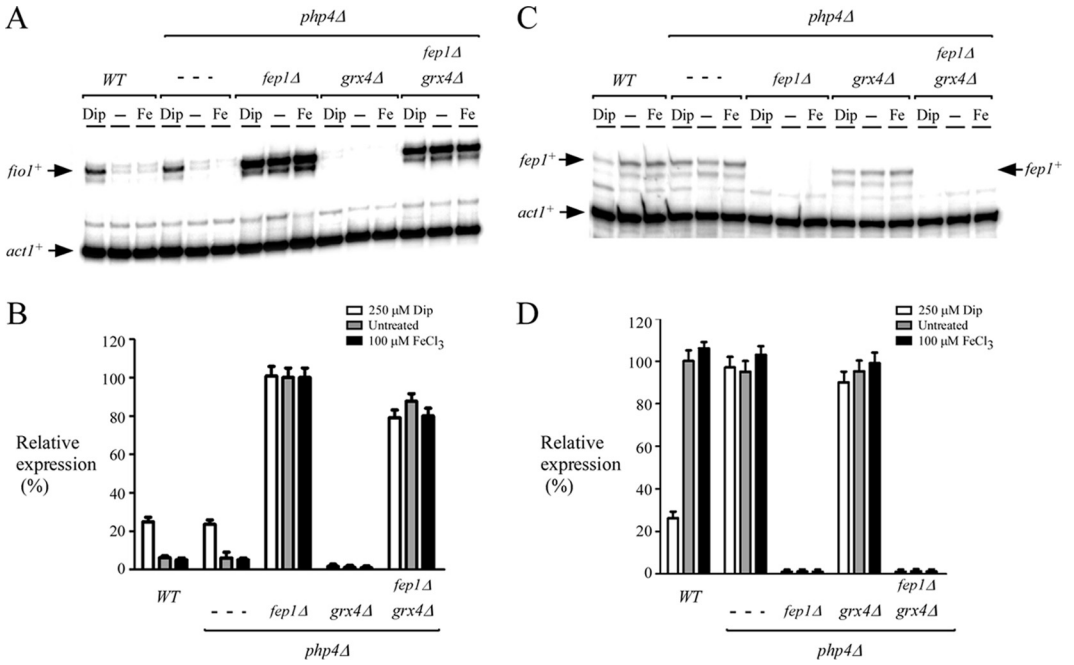

FIG. 1. *fio1*$^+$ transcript levels are constitutively repressed in a Fep1-dependent manner in a *php4*Δ strain lacking the *grx4*$^+$ allele. (A) The isogenic FY435 (wild-type [WT]), *php4*Δ, *php4*Δ *fep1*Δ, *php4*Δ *grx4*Δ, and *php4*Δ *fep1*Δ *grx4*Δ strains were grown to logarithmic phase. The cultures were left untreated (−) or were treated with Dip (250 μM) or $FeCl_3$ (Fe) (100 μM) for 90 min. Total RNA was prepared from each sample and then analyzed by RNase protection assays. Steady-state levels of *fio1*$^+$ and *act1*$^+$ mRNAs (indicated by the arrows) were analyzed in the indicated strains. (B) Graphic representation of the quantification of the results of three independent RNase protection assays, including the experiment shown in panel A. The values shown are the means of repeated experiments ± standard deviations. (C) Total RNA from the samples described in panel A was analyzed by RNase protection assays. The steady-state levels of *fep1*$^+$ and *act1*$^+$ mRNAs are indicated by the arrows. (D) Quantification of the *fep1*$^+$ transcript levels after the various treatments. The histogram values represent the averages of triplicate determinations ± standard deviations.

transcriptional regulation, we verified that the steady-state levels of *fep1*$^+$ in a wild-type strain were downregulated when the cells were grown under low-iron conditions and upregulated under basal and iron-replete conditions (Fig. 1C and D, WT). Therefore, the fact that the *fio1*$^+$ transcription was strongly repressed in *php4*Δ *grx4*Δ cells (even in the presence of Dip) suggested that Fep1 failed to respond to iron deficiency. These results further suggested that the elimination of Grx4 led to a constitutive activation of Fep1. Under these conditions, the genes under the control of Fep1 were repressed irrespective of the cellular iron status.

Dissociation of Fep1 from chromatin requires the Grx4 monothiol glutaredoxin. We tested the possibility that Grx4 regulated the function of Fep1 by interfering with its ability to bind to chromatin under iron-limiting conditions. We used a ChIP method to assess the levels of promoter occupancy by Fep1 in the absence or presence of Grx4. Cell lysates were prepared from *php4*Δ *fep1*Δ double or *php4*Δ *fep1*Δ *grx4*Δ triple mutant strains in which a functional *fep1*$^+$ gene containing a *TAP* tag inserted immediately after the initiator codon (TAP-Fep1) was returned by integration. Before cell lysate preparation, the strains were maintained under microaerobic conditions in the presence of the iron chelator Dip (100 μM). At mid-logarithmic phase, each cell culture was harvested, washed, and resuspended in a selective medium containing either Dip (250 μM) or $FeCl_3$ (250 μM) for 90 min. The results of the ChIP analysis showed that TAP-Fep1 occupied the *fio1*$^+$ promoter at high levels when *php4*Δ *fep1*Δ *grx4*Δ triple mutant cells had been cultured in the presence of iron or Dip (Fig. 2). Anti-mouse IgG antibodies immunoprecipitated 7.5-fold more TAP-Fep1 associated with the *fio1*$^+$ promoter DNA in *php4*Δ *fep1*Δ *grx4*Δ cells grown in the presence of Dip (250 μM) than in *php4*Δ *fep1*Δ *grx4*$^+$ cells grown under the same iron starvation conditions. When chromatin was prepared from *php4*Δ *fep1*Δ *grx4*Δ and *php4*Δ *fep1*Δ *grx4*$^+$ strains grown under iron-replete conditions, TAP-Fep1 pulled down elevated amounts of the *fio1*$^+$ promoter sequence compared to the intergenic region reference (Fig. 2). In the case of the *php4*Δ *fep1*Δ *grx4*$^+$ cells, TAP-Fep1 occupied the *fio1*$^+$ promoter at a maximum level (100%) under iron-replete conditions. Similarly, in the case of the *php4*Δ *fep1*Δ *grx4*Δ cells, we found that the association of TAP-Fep1 with the *fio1*$^+$ promoter was elevated, with an occupancy 4.3-fold higher than that of the *php4*Δ *fep1*Δ *grx4*$^+$ strain grown under low-iron conditions (Fig. 2). Parallel experiments using *php4*Δ *fep1*Δ cells provided evidence that any effects of either iron or Dip on TAP-Fep1 were independent of any potential changes in *TAP-fep1*$^+$ expression. As previously reported, and irrespective of whether or not the proteins were cross-linked to chromatin, TAP-Fep1 was clearly produced under both iron-limiting and iron-replete conditions (14; also data not shown). In addition, we found that cross-linked and un-cross-linked Fep1 was retained on IgG-Sepharose beads because the presence of TAP-Fep1 was detected in the immunoprecipitates obtained from cells grown in the ab-

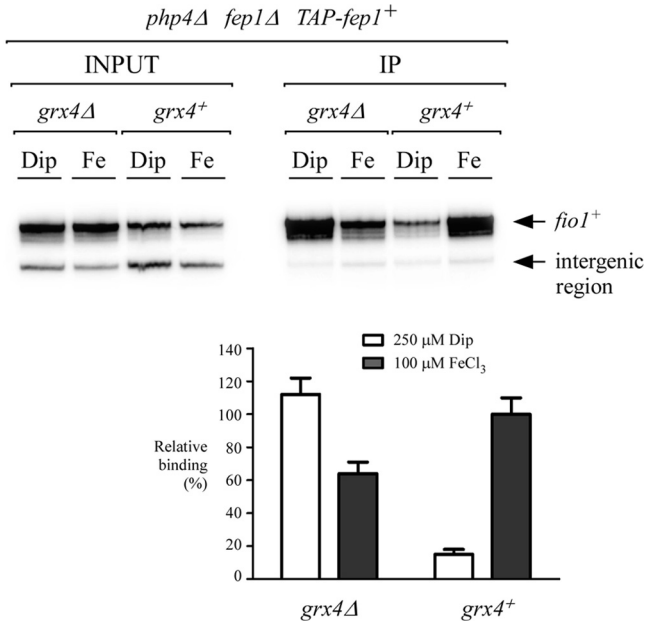

FIG. 2. Deletion of the *grx4*$^+$ gene results in a constitutive ability of TAP-Fep1 to bind to the *fio1*$^+$ promoter *in vivo*. ChIP analysis of the *fio1*$^+$ promoter in a *php4*Δ *fep1*Δ double mutant or a *php4*Δ *fep1*Δ *grx4*Δ triple mutant strain was performed. Both mutant strains were transformed with the integrative plasmid that encodes a functional TAP-tagged *fep1*$^+$ allele. The strains were precultured in the presence of 100 μM Dip, allowed to grow to an A_{600} of ~1.0, washed, and then incubated (90 min) in the presence of 250 μM Dip or 250 μM $FeCl_3$ (Fe). Chromatin was immunoprecipitated with anti-mouse IgG antibodies, and a specific region of the *fio1*$^+$ promoter was analyzed by PCR to determine Fep1 occupancy. The upper band represents the *fio1*$^+$-specific signal while the lower band is an internal background control derived from a nontranscribed region (i.e., the intergenic region). The lower panel shows a graphic representation of the quantitation of three independent ChIP assays, including the experiment depicted in the upper panel. The values shown are the means for three experiments ± standard deviations. The signals are expressed as percent relative binding and were calculated as a percentage of chromatin measured from the iron-treated *grx4*$^+$ strain (normalization to 100% corresponding to the values observed in the wild-type [*grx4*$^+$] strain under iron-replete conditions). Input, input chromatin; IP, immunoprecipitated chromatin.

sence or presence of iron (14; also data not shown). As expected, immunoprecipitates were not detectable in the case of *fep1*Δ *php4*Δ cells expressing the untagged *fep1*$^+$ allele (14; also data not shown). Taken together, the results indicated that, in the presence of Grx4, TAP-Fep1 associates with the *fio1*$^+$ promoter in iron-replete cells, whereas it dissociates from this promoter in response to iron starvation. In contrast, when Grx4 was deleted, the association between TAP-Fep1 and the *fio1*$^+$ promoter became sustained, allowing Fep1 to act as a constitutive repressor on its target gene regardless of iron availability.

Both Grx4 and Fep1 colocalize in the nucleus and physically interact with each other. Based on the data obtained, we asked whether the inactivation of Fep1 measured in the presence of Grx4 in iron-starved cells was intrinsically linked to an interaction between Grx4 and Fep1. To begin to address this point, we used a *php4*Δ *fep1*Δ *grx4*Δ triple mutant strain, in which case the functional integrative plasmids harboring *grx4*$^+$*-GFP* and *fep1*$^+$*-RFP* alleles were expressed under the control of the *grx4*$^+$ and *fep1*$^+$ promoters, respectively. As previously reported (6), Grx4-GFP fluorescence was detected in the whole cells with a predominance of the signal being observed in their nuclei (Fig. 3A). Furthermore, the pattern of Grx4-GFP fluorescence was similar in cells cultured under both iron starvation and iron-replete conditions (Fig. 3A). In the case of Fep1-RFP, the results revealed that the red fluorescent signal was observed in the nucleus in both iron-limited and iron-replete cells. It has been reported previously that Fep1 is a nuclear resident protein that can serve as a marker with which to probe the nucleus (14, 36). Merged images of both fluorescent fusion proteins showed that a proportion of the Grx4 protein colocalized with Fep1-RFP in the nucleus, suggesting that Grx4 could associate with the Fep1 iron-sensing transcription factor.

The colocalization of Grx4 and Fep1 led us to investigate the possibility that Grx4 associated with Fep1. Plasmids expressing either TAP alone and GFP-tagged Grx4 or TAP-tagged Fep1 and GFP-tagged Grx4 were cotransformed into a *php4*Δ *fep1*Δ *grx4*Δ triple mutant strain. These cells were grown to midlogarithmic phase, washed, and then incubated for 90 min in the presence of either 250 μM Dip or 100 μM $FeCl_3$. Total lysates were immunoprecipitated using IgG-Sepharose beads for the selective retrieval of TAP or the TAP-tagged proteins. Analysis of the proteins bound to the beads by immunoblotting with anti-GFP antibody showed that Grx4-GFP and TAP-Fep1 associated *in vivo* as Grx4-GFP was significantly enriched in the immunoprecipitates of TAP-Fep1 (Fig. 3B). Interestingly, the results showed that the formation of a heteroprotein complex between Grx4-GFP and TAP-Fep1 was independent of the iron status of the cells. A very weak background signal was observed when Grx4-GFP was probed in the bound fraction of control cells expressing only untagged TAP (Fig. 3B). To assess the steady-state levels of TAP or TAP-Fep1, immunoblot analyses of the protein preparations and coimmunoprecipitation reactions were performed using anti-IgG antibody (Fig. 3B). The specificity of the immunoprecipitation experiments was ascertained as follows. Total lysates and immunoprecipitates (or bound fractions) were analyzed by Western blotting using an antibody directed against PCNA, a soluble protein like the Grx4-GFP and TAP-Fep1 fusion proteins. The data showed (Fig. 3B) that PCNA was present in the total cell extracts but not in the immunoprecipitates. Collectively, these results revealed that immunoprecipitation of Grx4-GFP using anti-IgG antibody can be observed only when it is coexpressed with TAP-Fep1, indicating the formation of a heteroprotein complex between Grx4-GFP and TAP-Fep1. It must be emphasized that the formation of the heterocomplex was independent of the cellular iron status since similar levels of enrichment of Grx4-GFP were observed under both iron-depleted and iron-replete conditions.

As previously reported, the insertion of TAP at the N terminus of Fep1 does not interfere with its function (Fig. 3C) (14, 36). Indeed, *php4*Δ *fep1*Δ cells expressing a TAP-tagged *fep1*$^+$ allele were able to repress *fio1*$^+$ mRNA expression (~18- to 20-fold) under both standard (untreated) and iron-replete conditions. Importantly, *fio1*$^+$ mRNA levels in the *php4*Δ *fep1*Δ *grx4*Δ mutant strain coexpressing the *grx4*$^+$-GFP allele in conjunction with TAP-*fep1*$^+$ were also downregulated under basal (~17-fold) and iron-replete (~20-fold) conditions

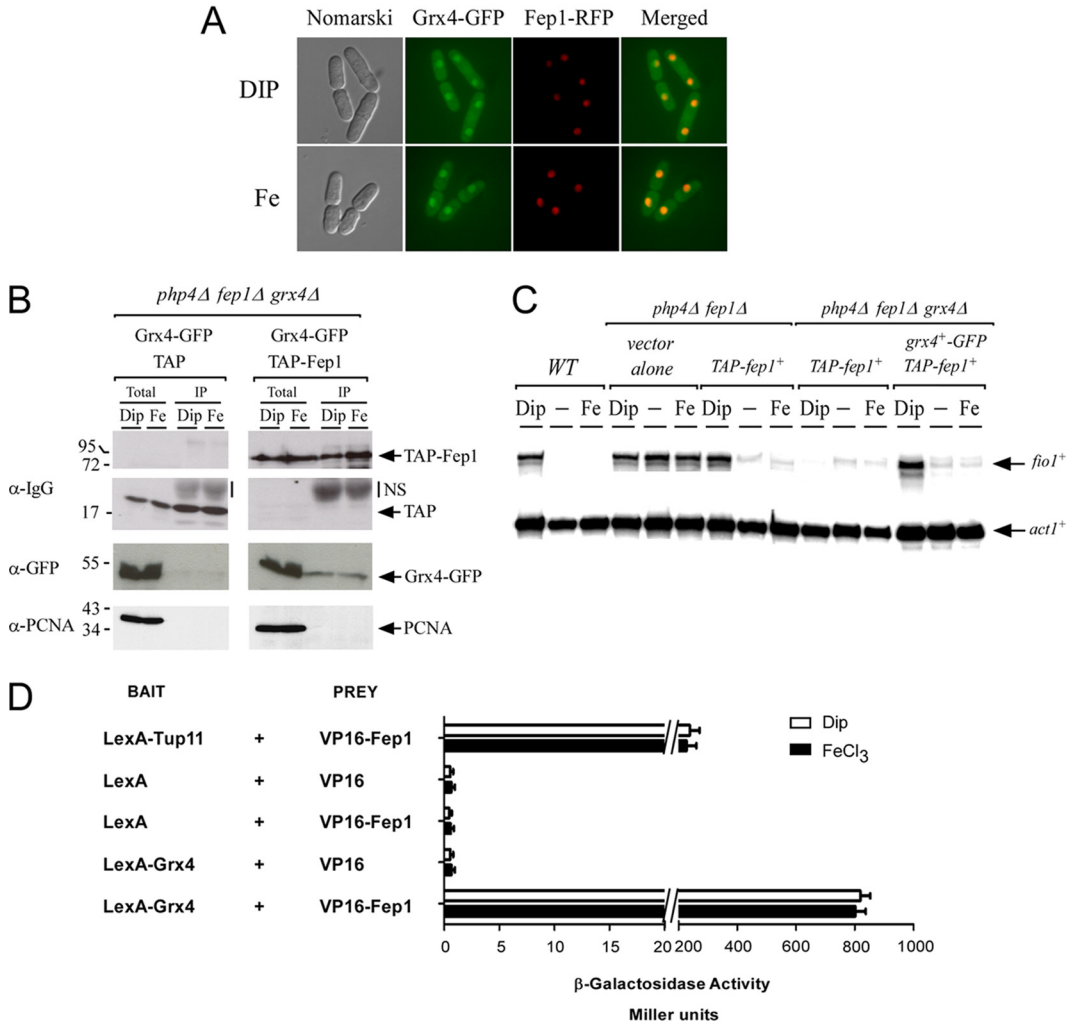

FIG. 3. *grx4* and *fep1* interact and colocalize to the nucleus. (A) *php4*Δ *fep1*Δ *grx4*Δ mutant cells were cotransformed with the integrative plasmids pJK-1200*grx4*$^+$*-GFP* and pBP*ade6-1478fep1*$^+$*-RFP*. Cells coexpressing the Grx4-GFP and Fep1-RFP fusion proteins were grown to logarithmic phase, and were then treated with either 250 μM Dip or 100 μM $FeCl_3$ (Fe) for 90 min. The cells were analyzed by fluorescence microscopy for both GFP (center left) and RFP (center right). Merged images are shown in the far right panels. Nomarski optics were used to examine cell morphology (far left panels). (B) *php4*Δ *fep1*Δ *grx4*Δ cells were cotransformed with plasmids expressing TAP alone and GFP-tagged Grx4 or TAP-tagged Fep1 and GFP-tagged Grx4. Extracts (Total) were subjected to immunoprecipitation (IP) using IgG-Sepharose beads. The beads were washed, and the eluted proteins were then analyzed by SDS-polyacrylamide gel electrophoresis. After electrophoresis, the bound proteins were analyzed by immunoblot assay using an anti-GFP antibody (α-GFP). A portion of the total cell extracts (~2%) was included to verify the presence of the immunoblotted proteins prior to chromatography. As additional controls, aliquots of whole-cell extracts and the bound fractions were probed with anti-mouse IgG antibody (α-IgG) and anti-PCNA antibody (α-PCNA). The positions of the protein standards are indicated on the left. NS, nonspecific signal. (C) Cointegration of the *grx4*$^+$*-GFP* and *TAP-fep1*$^+$ alleles in *php4*Δ *fep1*Δ *grx4*Δ mutant cells restores the iron-dependent regulation of *fio1*$^+$ expression. A *php4*Δ *fep1*Δ *grx4*Δ triple mutant strain was transformed with pJK148-1478NTAP*fep1*$^+$ or a combination of pJK148-1478NTAP*fep1*$^+$ and pJK210-1200*grx4*$^+$*-GFP*. Total RNA was isolated from both control (untreated) cells (−) and cells treated with Dip (250 μM) or $FeCl_3$ (100 μM). The steady-state levels of *fio1*$^+$ and *act1*$^+$ mRNA (indicated by the arrows) were determined. As additional controls, a *php4*Δ *fep1*Δ double mutant strain was transformed with an empty vector (vector alone) or a functional *TAP-fep1*$^+$ allele. The parent FY435 (WT) was used as a positive control for the repression of *fio1*$^+$ gene expression under iron-replete conditions. The results shown are representative of three independent experiments. (D) Using two-hybrid analysis, coexpression of the full-length Fep1 fused to VP16 with the LexA-Grx4 fusion protein produced high levels of β-galactosidase activity. The indicated bait and prey molecules were coexpressed in the *S. cerevisiae* strain L40 grown in the presence of $FeCl_3$ (100 μM) or under iron-deficient conditions (250 μM Dip). Liquid β-galactosidase activities (indicated in Miller units) were assayed in the L40 strain using an integrated (*lexAop*)$_8$*-lacZ* reporter. The values shown are the means for three replicates ± standard deviations. The LexA-Tup11 and VP16-Fep1 fusion proteins served as positive controls for the assay (51).

(Fig. 3C). We therefore concluded that when Grx4-GFP and TAP-Fep1 were coexpressed in *php4*Δ *fep1*Δ *grx4*Δ mutant cells, they functionally conferred iron-dependent regulation of *fio1*$^+$ expression in a manner similar to that of the wild-type Grx4 and Fep1 proteins in the parental strain (Fig. 3C).

To further investigate the association between Grx4 and Fep1, a two-hybrid analysis was performed using the full-length *grx4*$^+$ gene fused to the *lexA* coding region as bait and the *fep1*$^+$ gene fused to the coding region of the VP16 activation domain as prey. Coexpression of the full-length Grx4

fused to LexA with the VP16-Fep1 fusion protein resulted in the detection of high levels of β-galactosidase activity (~801 ± 58 Miller units) (Fig. 3D), indicating a very strong interaction between these two proteins. As positive controls, we used the LexA-Tup11 and VP16-Fep1 fusion proteins, which are known to strongly interact with each other (51). Coimmunoprecipitation experiments of *S. pombe* cell extracts suggested that the interaction between Grx4 and Fep1 was not modulated by iron (Fig. 3B). To determine whether the association between the LexA-Grx4 and VP16-Fep1 fusion proteins in baker's yeast was insensitive to iron in a manner that paralleled the coimmunoprecipitation results, the two full-length fusion proteins were coexpressed under both iron-limited and iron-replete conditions. The results of two-hybrid analysis showed that the full-length LexA-Grx4 and VP16-Fep1 proteins associate with each other in an iron-independent manner, resulting in very high levels of β-galactosidase activity in both cases (Fig. 3D).

Grx4 interacts strongly with the C-terminal region of Fep1 but associates only weakly with its N-terminal region. Because analogous results were obtained using both methods of protein-protein interaction analysis, we used the two-hybrid technology to delineate the region(s) of Fep1 that predominantly interacted with Grx4. We first investigated the possibility of interaction between Grx4 with the N-terminal residues 2 to 241 and 2 to 359 of Fep1 (^{2}Fep1^{241} and ^{2}Fep1^{359}, respectively) and the C-terminal 323 amino acid residues of Fep1 (residues 242 to 564 [^{242}Fep1^{564}]). β-Galactosidase assays of VP16-^{2}Fep1^{241} and VP16-^{2}Fep1^{359} coexpressed with LexA-Grx4 revealed only weak activity levels (7.1 ± 1.9 and 14.9 ± 1.6 Miller units, respectively). However, these levels of β-galactosidase activity were significantly higher than the background values of pairs of noninteracting proteins (Fig. 4A). We then tested whether the C-terminal region of residues 242 to 564 of Fep1 was involved in the interaction with Grx4. In these experiments, VP16-^{242}Fep1^{564} showed very high levels of β-galactosidase activity (742 ± 112 Miller units), similar to the activity observed with the full-length VP16-Fep1 fusion protein (664 ± 83 Miller units) (Fig. 4A). Immunoblot analyses of protein extracts using anti-LexA and anti-VP16 antibodies clearly indicated that the fusion proteins were expressed in the cotransformed cells (Fig. 4B). Although we consistently detected LexA alone, full-length LexA-Grx4 protein, VP16-Fep1 protein, and its truncated derivatives, we were unable to detect the VP16 polypeptide alone. This observation may be due to its very low predicted molecular mass (~8 kDa). Overall, the results suggested that the C-terminal region encompassing amino acids 242 to 564 of Fep1 is needed to form a stable interaction with Grx4.

To gain additional insight into the C-terminal region of residues 242 to 564 of Fep1 that was responsible for interaction with Grx4, seven chimeric proteins were generated using different segments of the Fep1 protein. These segments comprised residues 319 and 564 (VP16-^{319}Fep1^{564}), 405 to 564 (VP16-^{405}Fep1^{564}), 432 to 564 (VP16-^{432}Fep1^{564}), 405 to 541 (VP16-^{405}Fep1^{541}), 405 to 501 (VP16-^{405}Fep1^{501}), 405 to 480 (VP16-^{405}Fep1^{480}), and 405 to 457 (VP16-^{405}Fep1^{457}). β-Galactosidase assays of VP16-^{432}Fep1^{564} or VP16-^{405}Fep1^{457} coexpressed with LexA-Grx4 showed only very weak activity levels (1.1% and 0.9%, respectively) relative to that of the VP16-^{242}Fep1^{564} fusion protein (Fig. 5A). In contrast, constructs encoding VP16-^{319}Fep1^{564}, VP16-^{405}Fep1^{564}, VP16-^{405}Fep1^{541}, and VP16-^{405}Fep1^{501} had high levels of β-galactosidase activity (97%, 118%, 106%, and 102%, respectively) that were similar to the level of VP16-^{242}Fep1^{564} (Fig. 5). Coexpression of VP16-^{405}Fep1^{480} with LexA-Grx4 exhibited significantly reduced levels of β-galactosidase activity; specifically, levels were reduced to 29% of the level of the VP16-^{242}Fep1^{564} fusion protein (Fig. 5). Importantly, the interaction between LexA-Grx4 and the VP16-^{242}Fep1^{564}, VP16-^{319}Fep1^{564}, VP16-^{405}Fep1^{564}, VP16-^{405}Fep1^{541}, VP16-^{405}Fep1^{501}, or VP16-^{405}Fep1^{480} fusion proteins using two-hybrid analysis was not found to be modulated by iron availability (data not shown). All fusion proteins tested for two-hybrid interactions were detected by immunoblot analyses, except the chimeric VP16-^{405}Fep1^{480} and VP16-^{405}Fep1^{457} proteins (Fig. 5B). Given this situation, we assayed the levels of mRNA expression of *VP16* alone and *VP16-fep1*$^{+}$ fusion constructs (full-length and the truncated derivatives) using RNase protection assays. The results showed that *VP16* used without or with the wild-type or truncated *fep1* constructs was clearly expressed, with transcripts being detected in the case of each prey construct (Fig. 5C). Based on the two-hybrid assay, we concluded that the C-terminal segment of Fep1 encompassing amino acid residues 242 to 564 is required for a full-strength interaction with Grx4. Furthermore, within this region, a domain corresponding to amino acids 405 to 501 constitutes a minimal module that is sufficient for maximal interaction between Fep1 and Grx4.

Two domains of Grx4 are involved in the interaction with Fep1, but only the GRX domain interacts in an iron-dependent manner with the N-terminal region of Fep1. The identification of the amino acid regions of Fep1 required for its association with Grx4 prompted elucidation of the region on Grx4 that was necessary for this interaction. The monothiol glutaredoxin Grx4 from the fission yeast *S. pombe* includes two major domains that exhibit a high overall sequence homology with most family members of monothiol glutaredoxins (11). These two domains are denoted thioredoxin (TRX)-like and glutaredoxin (GRX)-like. The N-terminal TRX-like domain of Grx4 contains a WAAPC^{35}K sequence that is reminiscent of the thioredoxin active site motif WCGPCK (11). The C-terminal GRX-like domain of Grx4 contains the highly conserved residues C^{172}GFS that are required for monothiol glutaredoxin cellular functions (11). We designed truncated segments of the N- and C-terminal ends of Grx4, leaving only its GRX and TRX domains, respectively. The construct in which the TRX domain of Grx4 was removed (LexA-^{105}Grx4^{244}) did not exhibit β-galactosidase activity when it was coexpressed with VP16-^{405}Fep1^{501} (Fig. 6A). This result suggested that the TRX domain was needed to interact with the C-terminal region of residues 405 to 501 of Fep1. Importantly, the chimeric LexA-^{2}Grx4^{142} (domain TRX) molecule displayed a 6% decrease in the activity of the reporter β-galactosidase compared to that of the full-length LexA-^{2}Grx4^{244} fusion protein (Fig. 6A). However, when the Cys^{35} residue located within the TRX domain (LexA-Grx4 C35A mutant) was mutated, β-galactosidase activity was abolished. Consistent with the fact that the TRX domain was required for the association between Grx4 and the Fep1 C-terminal region, when the Cys^{172} residue located within the GRX domain was mutated, the reporter β-galactosidase was still highly expressed (93%). We then investigated whether the ability of the TRX domain of Grx4 to interact with the C-ter-

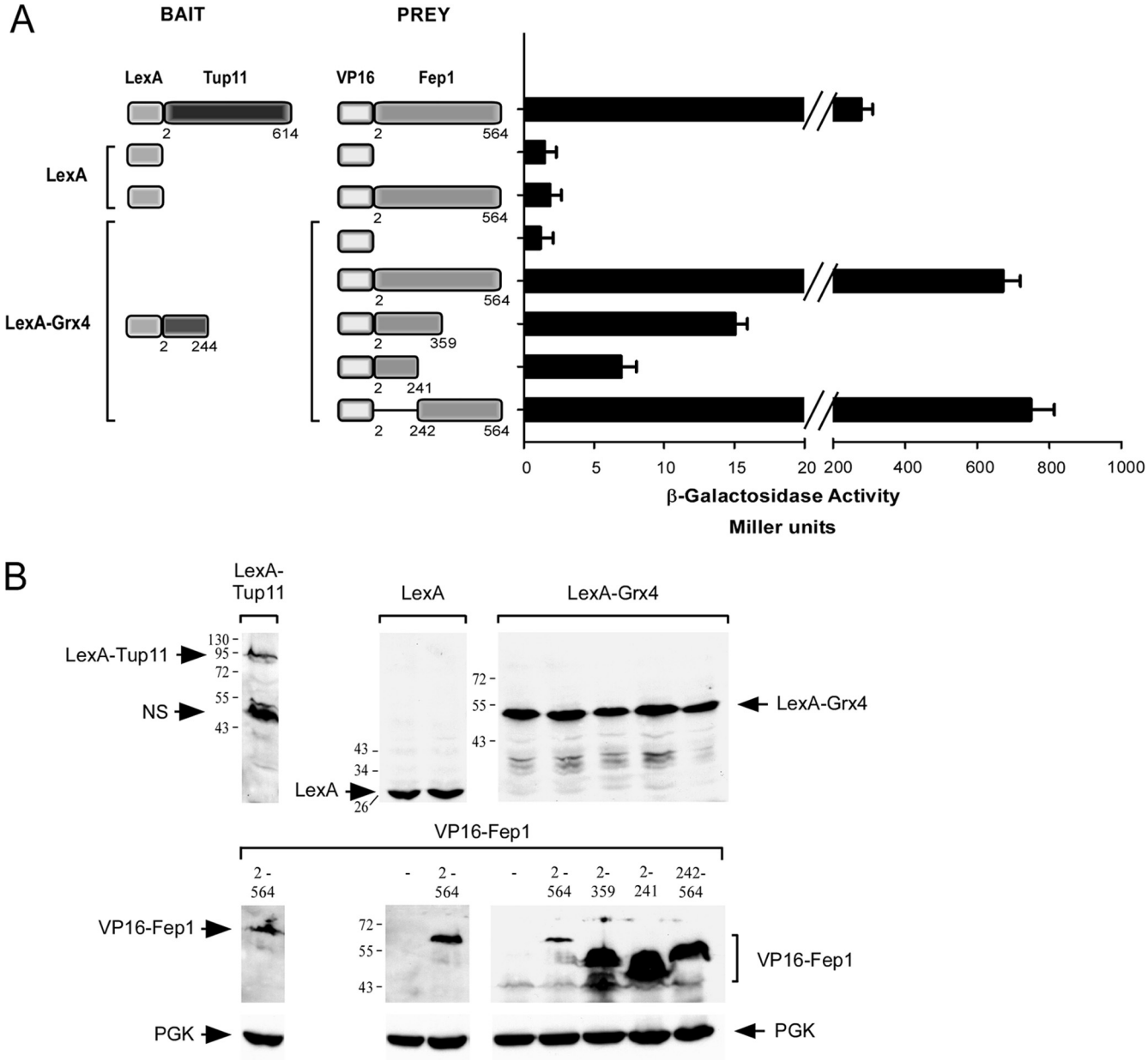

FIG. 4. The N- and C-terminal regions of Fep1 interact with Grx4, with the latter region making a much stronger interaction than the former. (A) The LexA-Grx4 fusion protein was coexpressed with the full-length VP16-Fep1 protein or its truncated derivatives. The amino acid sequences of the Grx4, Fep1, and Tup11 proteins are numbered relative to their first initiator codons. Each set of constructs was coexpressed in the *S. cerevisiae* strain L40 under basal conditions. As a measure of protein-protein interactions, liquid β-galactosidase assays were carried out, and the results shown are the means of triplicate determinations ± standard deviations. The LexA-Tup11 and VP16-Fep1 fusion proteins were used as positive controls (51). (B) Cell lysates from aliquots of the cultures described in panel A were analyzed by immunoblotting with anti-LexA, anti-VP16, or anti-phosphoglycerate kinase (PGK) (as an internal control) antibodies. The positions of protein standards are indicated to the left. NS, nonspecific signal.

minal region of Fep1 was affected by iron. Results showed that the interaction between the TRX domain of Grx4 and the amino acid region consisting of residues 405 to 501 of Fep1 was independent of the iron status (Fig. 6A). To ensure that the LexA-Grx4 protein and its mutant derivatives, as well as the chimeric VP16-^{405}Fep1^{501} molecule, were expressed in the cotransformed cells, immunoblot analyses of protein extracts were carried out using both anti-LexA and anti-VP16 antibodies. Chimeric proteins were detected under conditions of both low and high levels of iron (Fig. 6B).

Two-hybrid analyses (Fig. 4) showed that coexpression of the full-length LexA-Grx4 with the VP16-^{2}Fep1^{359} protein produced low, but significant, levels of β-galactosidase activity (14.9 ± 1.6 Miller units), indicating an interaction between Grx4 and the Fep1 amino acid fragment consisting of residues 2 to 359. To further delineate the region of Grx4 that inter-

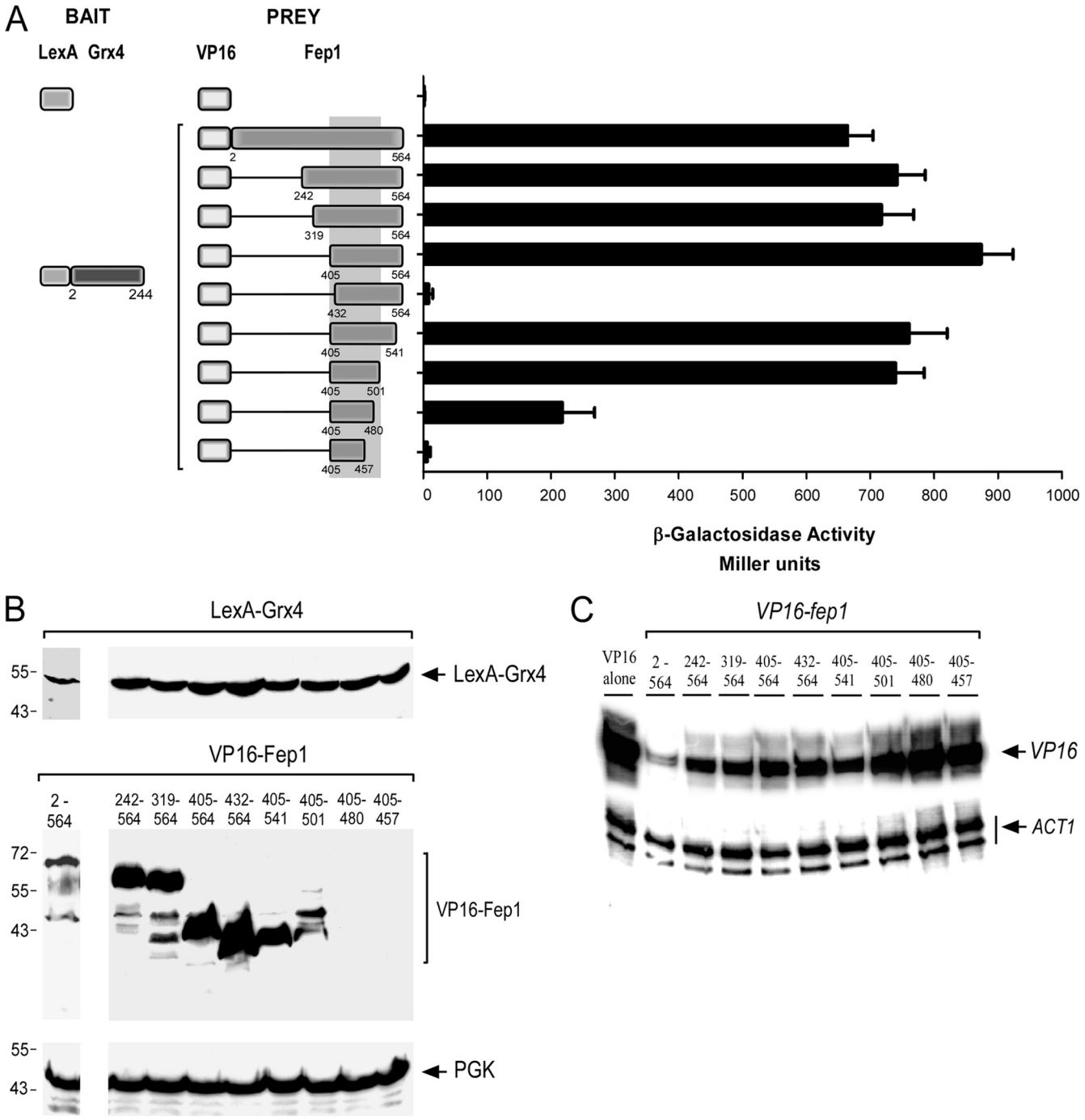

FIG. 5. Minimal C-terminal region of Fep1 that is required for interaction with the LexA-Grx4 fusion protein in the two-hybrid assays. (A) The LexA-Grx4 fusion protein was coexpressed with a series of truncated versions of VP16-Fep1 in the L40 strain. Positive interactions between the proteins were detected by liquid β-galactosidase assays. The histogram values represent the averages of triplicate determinations ± standard deviations. (B) The LexA-Grx4 fusion protein and the truncated versions of the VP16-Fep1 fusion proteins were detected by immunoblotting using anti-LexA and anti-VP16 antibodies, respectively. As a control, total extract preparations were probed with an anti-PGK antibody. (C) Aliquots of the cultures described for panel A were also examined by RNase protection assay for steady-state levels of the *VP16* transcripts. Actin (*ACT1*) mRNA levels were probed as an internal control.

acted with the N-terminal region of residues 2 to 359 of Fep1, we created four different chimeric LexA-Grx4 molecules, LexA-^{2}Grx4^{142} (domain TRX), LexA-^{105}Grx4^{244} (domain GRX), LexA-Grx4 with the mutation C172A [LexA-Grx4(C172A)], and LexA-Grx4(C35A). The LexA-^{2}Grx4^{244}, LexA-^{105}Grx4^{244} (domain GRX), and LexA-Grx4(C35A) fusion proteins produced significant levels of β-galactosidase activity (23.8 ± 1.1, 20.5 ± 2.1, and 20.1 ± 2.2 Miller units,

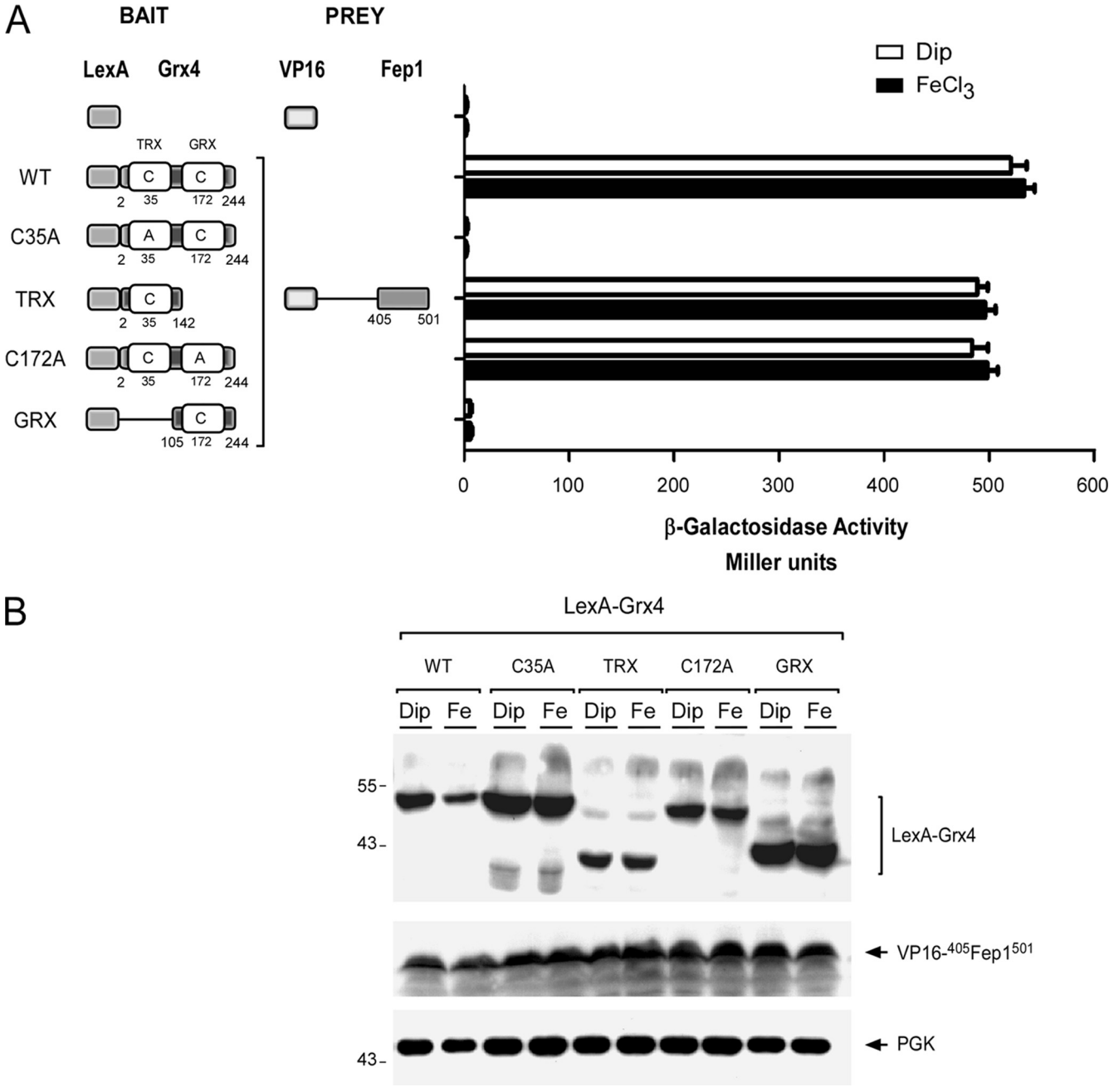

FIG. 6. The TRX domain of Grx4 is required for its interaction with the C-terminal region of Fep1. (A) Schematic illustration of the LexA-Grx4 fusion protein and its mutant derivatives. The N-terminal 142 amino acid residues of Grx4 encompass its TRX domain, while residues 105 to 244 of Grx4 contain the GRX domain. The point mutations are marked with an A (instead of the wild-type C residues). The amino acid sequence numbers refer to the positions relative to the first amino acid of each protein. Cotransformed cells were grown under iron-deficient conditions (250 μM Dip) or in the presence of iron (100 μM $FeCl_3$). Protein-protein interactions were detected by liquid β-galactosidase assays and are indicated in Miller units. The error bars indicate the standard deviations of triplicate samples. (B) Whole-cell extracts were prepared from aliquots of the cultures described in panel A and were analyzed by immunoblotting using either anti-LexA or anti-VP16 antibody. As an internal control, total extract preparations were probed with an anti-PGK antibody.

respectively) under conditions of low iron levels when coexpressed with VP16-^{2}Fep1^{359} (Fig. 7A). In contrast, when these three cotransformants were incubated in the presence of iron, β-galactosidase activity decreased by 75%, 77%, and 78%, respectively (Fig. 7A). When the GRX domain was removed (LexA-^{2}Grx4^{142}) or mutated [LexA-Grx4(C172A)] and then tested for interaction with VP16-^{2}Fep1^{359}, no significant β-galactosidase activity was detected, irrespective of the cellular iron status. Western blot analysis revealed equivalent expression levels of the LexA-Grx4 fusion protein and its derivatives, regardless of the iron status (Fig. 7B). Based on these data, we concluded that the Grx4 GRX domain interacts with the N

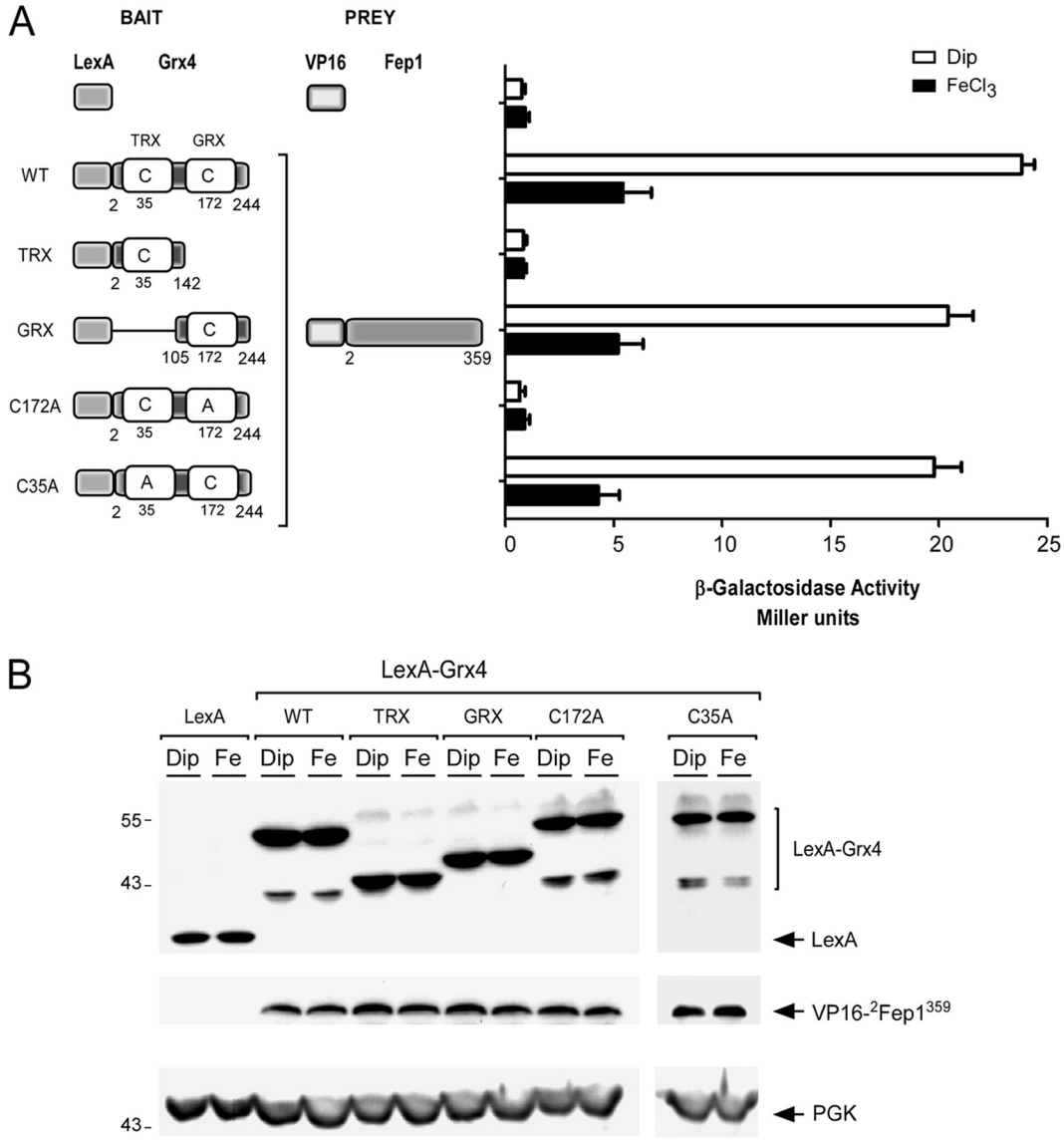

FIG. 7. High concentrations of iron strongly decrease the interaction between the Grx domain of Grx4 and the N-terminal region of Fep1. (A) Both the truncated and mutated LexA-Grx4 fusion proteins used as baits are depicted (see the legend of Fig. 6A for an explanation of the schematic). The indicated Fep1 N-terminal region (residues 2 to 359) was coexpressed with the VP16 activation domain as a prey. Cotransformed cells were grown to an A_{600} of 0.3 and then were treated with Dip (250 μM) or $FeCl_3$ (100 μM) for 4 h. Liquid β-galactosidase assays were carried out as a measure of protein-protein interactions. The values shown are the averages of triplicate determinations ± standard deviations. (B) Protein extracts were prepared from aliquots of the cultures used in panel A and were then analyzed by immunoblotting using either anti-LexA, anti-VP16, or anti-PGK (as an internal control) antibody.

terminus of Fep1 in an iron-dependent manner. Furthermore, the Cys^{172} residue within the GRX domain of Grx4 is absolutely required as its removal abrogates the physical interaction between the LexA-Grx4 and VP16-^{2}Fep1^{359} fusion proteins.

Based on the data obtained (Fig. 6 and 7), the full-length VP16-Fep1 fusion protein was tested for interaction with separate domains of Grx4 as a function of iron availability. Although the strength of the interaction between the GRX domain (LexA-^{105}Grx4^{244}) and VP16-^{2}Fep1^{564} was low (~23.0 ± 2.0 Miller units), based on β-galactosidase activity, it was significantly higher than the interactions of the negative controls (which consist of vectors only). In addition, we observed that high concentrations of iron resulted in a decrease in β-galactosidase activity (~48%), revealing a weaker interaction of the GRX domain with Fep1 (Fig. 8A). Similarly, the mutant LexA-Grx4(C35A) (in which the TRX domain was mutated) exhibited a decreased (~47%) physical interaction with Fep1 in the presence of high levels of iron (Fig. 8A). In subsequent assays, coexpression of the TRX domain (LexA-^{2}Grx4^{142}) with the VP16-^{2}Fep1^{564} fusion protein produced cotransformants exhibiting high levels of β-galactosidase activity that were not modulated by iron (Fig. 8A). Analogous to the interaction between the TRX domain and Fep1, cells coexpressing LexA-Grx4(C172A) (in which the GRX domain was mutated) and

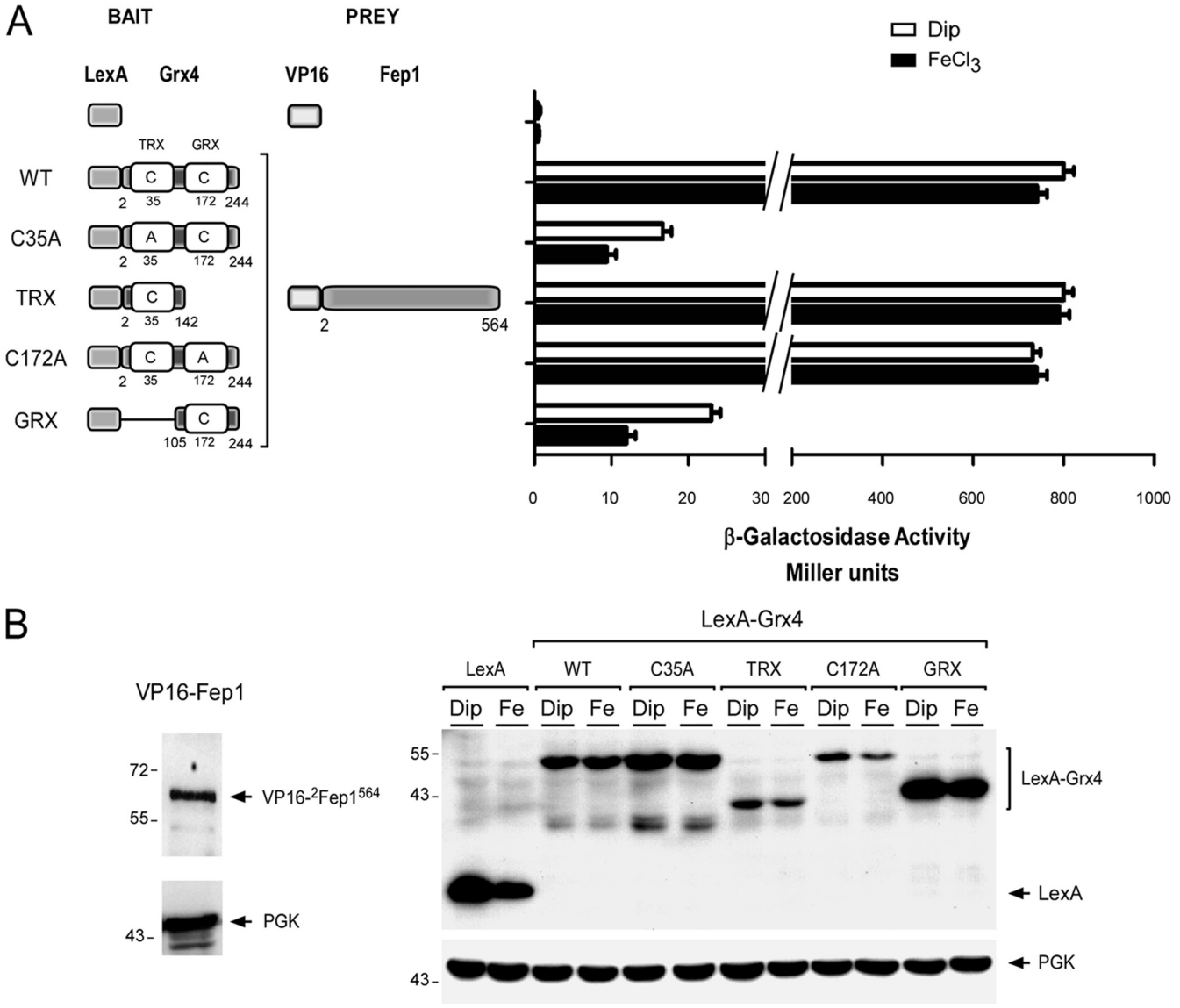

FIG. 8. The TRX domain of Grx4 strongly associates with the full-length Fep1 protein, whereas a weak, but reproducible, interaction between Fep1 and the GRX domain is detected, and is enhanced under low iron conditions. (A) Schematic diagrams of the LexA DNA binding domain either alone or the LexA-Grx4 fusion protein and its mutant derivatives (see the legend of Fig. 6A for an explanation of the schematic). The indicated bait molecule was coexpressed with the VP16 activation domain or the full-length VP16-Fep1 fusion protein. Cotransformed cells were grown to an A_{600} of 0.3 and were then incubated under iron-deficient conditions (250 μM Dip) or with excess iron (100 μM) for 4 h. Protein-protein interactions were assessed by liquid β-galactosidase assays, and the results are indicated in Miller units. The error bars indicate the standard deviations of samples analyzed in triplicate. (B) Total cell extract preparations from aliquots of the cultures used in the assays described in panel A were analyzed by immunoblotting using anti-LexA, anti-VP16, or anti-PGK antibody. For simplicity, the full-length VP16-Fep1 fusion protein was analyzed in iron-deficient cells since its expression level detected in the iron-replete cells was virtually identical.

VP16-^{2}Fep1^{564} exhibited very high levels of β-galactosidase activity that were independent of the iron status (Fig. 8A). Western blot analyses of protein extracts using anti-LexA and anti-VP16 antibodies showed that the fusion proteins were expressed in the cotransformed cells independently of the iron levels (Fig. 8B).

Fep1 function is inactivated through the action of the GRX domain under conditions of iron starvation. Given the fact that two-hybrid assays showed that the strength of the interaction between the two Grx4 domains and Fep1 were different, we further investigated the effect of these domains on Fep1 function. These experiments were in keeping with the fact of the importance of the regulation of *fio1*$^{+}$, a gene known to encode a component of the iron transport machinery. Plasmids expressing the mutant proteins (Fig. 9) were transformed into an *S. pombe php4*Δ *fep1*Δ *grx4*Δ strain. In addition, each transformant coexpressed the Fep1-RFP fusion protein that served as a marker of nuclei. The Grx4(C35A)-GFP, ^{1}Grx4^{142}-GFP, and Grx4(C172A)-GFP fusion proteins were detected in the nucleus and the cytoplasm (Fig. 9A, C35A, TRX, and C172A). Importantly, the nuclear portion of all three of the above-mentioned Grx4 mutant proteins colocalized with the Fep1-

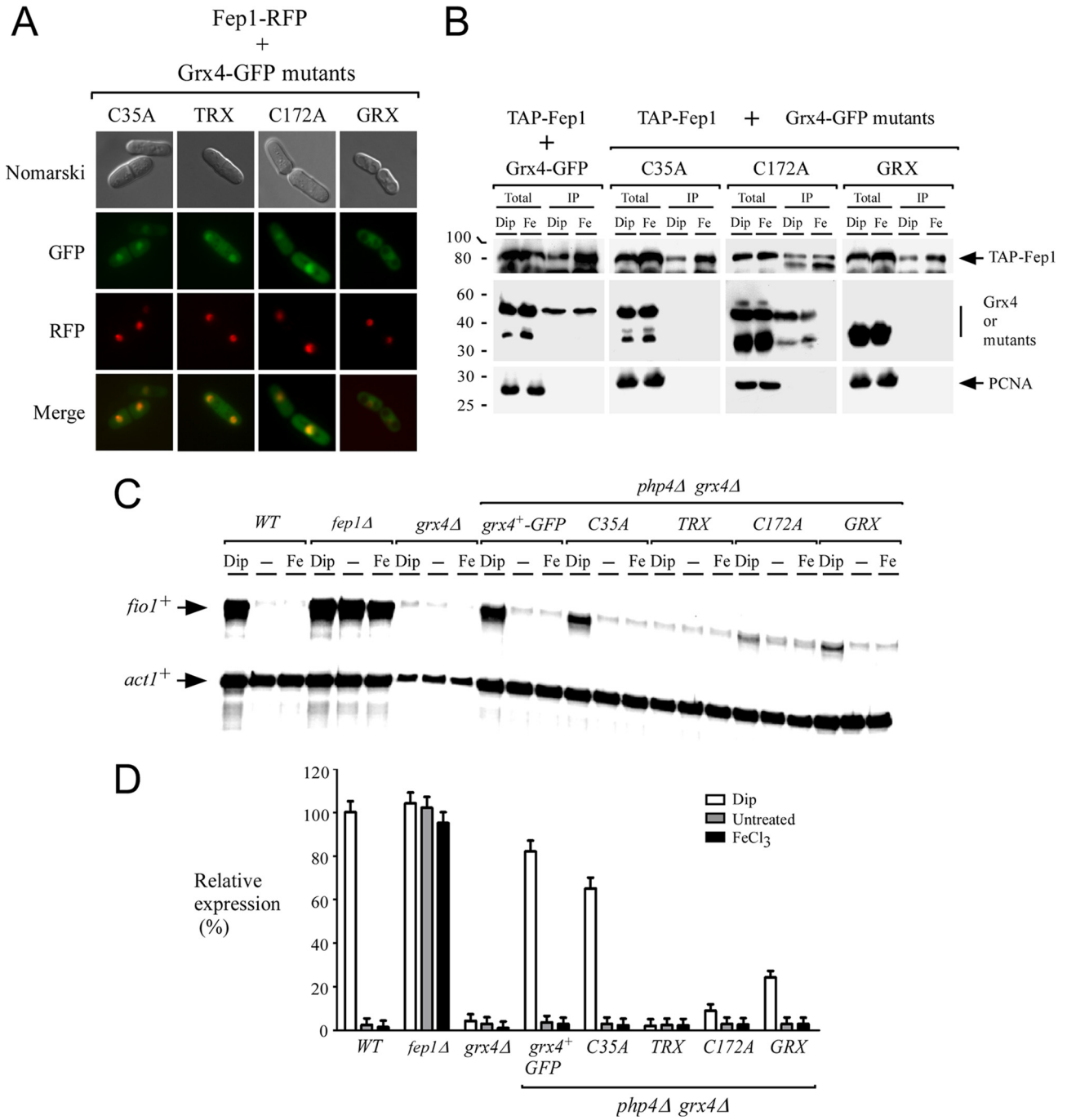

FIG. 9. The TRX domain is required for the maximal in vivo association between Grx4 and Fep1, while the GRX domain is necessary for the inhibition of Fep1 activity in response to iron deficiency. (A) *php4*Δ *fep1*Δ *grx4*Δ cells containing a functional *fep1*$^{+}$*-RFP* allele were transformed with *grx4*(*C35A*)*-GFP* (C35A), ^{1}*grx4*^{142}*-GFP* (TRX), *grx4*(*C172A*)*-GFP* (C172A), or ^{105}*grx4*^{244}*-GFP* (GRX). The cells were analyzed by fluorescence microscopy so as to reveal both RFP and GFP expression and were then examined by Nomarski microscopy for cell morphology. Merged images of Fep1-RFP coexpressed with the indicated *grx4* mutants are shown (bottom panels). (B) Cells harboring a *php4*Δ *fep1*Δ *grx4*Δ triple deletion were cotransformed with *TAP-fep1*$^{+}$ plus *grx4*$^{+}$*-GFP*, *TAP-fep1*$^{+}$ plus *grx4*(*C35A*)*-GFP* (C35A), *TAP-fep1*$^{+}$ plus *grx4*(*C172A*)*-GFP* (C172A), or *TAP-fep1*$^{+}$ plus ^{105}*grx4*^{244}*-GFP* (GRX). Mid-logarithmic-phase cultures were incubated in the presence of Dip (250 μM) or $FeCl_3$ (100 μM) (Fe) for 90 min. Lysates (total) were incubated with an IgG-Sepharose resin. Following washing, the bound fractions were analyzed by immunoblotting using the anti-GFP antibody. As controls, aliquots of both the cell lysates and bound fractions were probed with an anti-mouse IgG antibody and an anti-PCNA antibody. A portion of the total protein lysates (~2%) was also analyzed to verify the presence of the immunoblotted proteins prior to chromatography. (C) RNase protection analysis of the *fio1*$^{+}$ transcript levels in wild-type (WT), *fep1*Δ, *grx4*Δ, and *php4*Δ *grx4*Δ strains exposed to 250 μM Dip or 100 μM $FeCl_3$ or left untreated (−). Cells harboring a *php4*Δ *grx4*Δ double deletion were transformed with the *grx4*$^{+}$*-GFP*, *grx4*(*C35A*)*-GFP* (C35A), ^{1}*grx4*^{142}*-GFP* (TRX), *grx4*(*C172A*)*-GFP* (C172A), or ^{105}*grx4*^{244}*-GFP* (GRX) alleles. The steady-state levels of the *fio1*$^{+}$ and *act1*$^{+}$ mRNAs are indicated with arrows. (D) Quantification of the *fio1*$^{+}$ transcript levels after the various treatments. The histogram values represent the averages of triplicate determinations ± standard deviations.

RFP fusion protein. Interestingly, the ^{105}Grx4^{244}-GFP mutant, which expressed only the Grx domain, was predominantly observed in the cytoplasm (Fig. 9A). Only a very small fraction of ^{105}Grx4^{244}-GFP colocalized with the Fep1-RFP protein in the nucleus (Fig. 9A). We then examined whether mutated forms of Grx4 affected its ability to interact with Fep1 in *S. pombe*. We coexpressed TAP-Fep1 with the GFP tag fused to either the C-terminal region of Grx4 or its mutant derivatives. Each combination was coexpressed in a *php4*Δ *fep1*Δ *grx4*Δ mutant strain, and coimmunoprecipitation experiments were performed in cells cultured in the presence of either the iron chelator Dip or $FeCl_3$ (Fig. 9B). Western blot analysis of the proteins retained by the beads (bound fraction) using an anti-GFP antibody revealed that both wild-type Grx4-GFP and Grx4(C172A)-GFP were present in the immunoprecipitate fraction under iron-limiting and iron-replete conditions (Fig. 9B). In contrast, and regardless of the iron levels, neither Grx4(C35A)-GFP nor ^{105}Grx4^{244}-GFP was found in the bound fraction of cells expressing the full-length TAP-Fep1 protein (Fig. 9B, C35A and GRX). Notably, weak protein-protein interactions might not be detectable using the less-sensitive coimmunoprecipitation method, especially compared to the exquisitely sensitive yeast two-hybrid method. The specificity of the coimmunoprecipitation experiments was ascertained using total cell lysates. Proteins retained by the beads were analyzed by Western blotting using an antibody directed against PCNA, a soluble protein like TAP-Fep1, Grx4-GFP, or its mutant derivatives. PCNA was found to be present in the total cell extracts but not in the retained protein fraction (Fig. 9B). Furthermore, interaction between the Grx4-GFP and TAP proteins was not observed when TAP was coexpressed alone with the GFP tag fused to Grx4 (Fig. 3B and data not shown). To assess the steady-state protein levels of TAP-Fep1, immunoblot analyses of both the protein preparations and the bound fractions were carried out using anti-IgG antibody (Fig. 9B). Together, the coimmunoprecipitation data show that the TAP-Fep1 and either the Grx4-GFP or the Grx4(C172A)-GFP fusion proteins specifically interacted with each other to form a stable heteroprotein complex that could be pulled down from whole-cell extracts.

To assess the effect of the expression of different Grx4 mutants on Fep1 function, we carried out RNase protection analysis to examine the relative transcriptional profile of the Fep1-regulated target gene *fio1*$^+$ (Fig. 9C). *php4*Δ *grx4*Δ cells expressing the ^{1}Grx4^{142}-GFP (TRX domain) mutant, in which the GRX domain was absent, displayed a constitutive repression of *fio1*$^+$ irrespective of the iron status. Similarly, when *php4*Δ *grx4*Δ mutant cells were transformed with the *grx4*(*C172A*) allele (in which the conserved Cys^{172} of the glutaredoxin active site was substituted for an Ala residue), *fio1*$^+$ transcripts were still largely repressed, even in the presence of Dip, indicating that the Fep1 repressor failed to respond to low-iron conditions. Surprisingly, *php4*Δ *grx4*Δ cells expressing the *^{105}grx^{244}-GFP* (GRX) allele displayed a low, but significant, increase (8.2-fold) in *fio1*$^+$ transcript levels in the presence of Dip compared to the *^{1}grx4^{142}-GFP* (TRX) allele expressed under the same conditions (Fig. 9C). Moreover, *php4*Δ *grx4*Δ cells expressing *grx4*(*C35A*)-*GFP* and *grx4*$^+$-*GFP* alleles consistently showed an iron-dependent regulation of the *fio1*$^+$ gene. *fio1*$^+$ mRNA levels were induced (21.8- and 22.2-fold, respectively, compared with basal levels of expression observed in untreated cells) in cells cultured in the presence of Dip, whereas in both untreated and iron-replete cells, *fio1*$^+$ transcript levels were repressed as in the case of the wild-type strain (Fig. 9C). As expected, *fio1*$^+$ transcript levels were increased only in wild-type cells cultured in the presence of Dip (33.1-fold) compared with the level of transcripts detected from control (untreated) cells. *fio1*$^+$ expression was constitutively repressed in a *grx4*Δ single mutant strain, whereas *fio1*$^+$ mRNA levels were strongly increased in a *fep1*Δ single mutant strain (Fig. 9C). Taken together, these findings supported the interpretation that the strong interaction between the C terminus of Fep1 and the TRX domain of Grx4 is not necessary for iron limitation-dependent inhibition of Fep1. In contrast, the weaker interaction between the N terminus of Fep1 and the GRX domain of Grx4 appears to play a critical role for inactivation of Fep1 function in response to iron starvation.

DISCUSSION

Excess iron accumulation in the fission yeast *S. pombe* triggers the transcription factor Fep1 to repress the expression of the genes involved in the acquisition of iron (15, 21, 35). In contrast, when these cells undergo a transition from conditions of iron sufficiency to iron deficiency, the activity of Fep1 must be shut down to allow *de novo* synthesis of high-affinity iron transporters. Although the mechanism by which Fep1 is inactivated by iron starvation is crucial, the molecular components and features that dictate how Fep1 is inhibited are still poorly understood. Our group has already identified one mechanism that operates at the transcriptional level (28). We determined that *fep1*$^+$ gene expression is under the control of the CCAAT-binding factor Php4 and that its expression is downregulated under conditions of iron starvation (>0.01 μM) and upregulated under conditions of both low (0.74 μM) and high levels (100 μM) of iron (28). In the present study, we have identified a second mechanism that takes place at the posttranslational level. Using a biological system in which the Php4 protein was absent, thus allowing us to unlink iron starvation-dependent behavior of the Fep1 protein from its transcriptional regulation by Php4, we determined that the presence of a functional *grx4*$^+$ gene was required to inactivate Fep1 in response to iron deficiency. This result was rather unexpected since monothiol glutaredoxins are known to inhibit iron-regulatory transcription factors in response to excess iron but not under conditions of iron deficiency. For instance, it is known that the *S. cerevisiae* transcription factor Aft1 activates high-affinity iron transport gene expression in response to iron deficiency. In contrast, Aft1 is inactivated by iron repletion (48, 49). Although the precise mechanism of iron-dependent inhibition of Aft1 activity remains unclear, it has been shown that the presence of different cellular components, including glutathione, the Fra1 and Fra2 proteins, and the monothiol glutaredoxins Grx3 and Grx4, are required to communicate cellular iron levels to Aft1 as well as to inhibit its function upon iron repletion (15). It has been shown that Grx3 and Grx4 interact directly with Aft1 (20, 32, 38). However, the association of Grx3 and Grx4 with Aft1 was shown to be independent of the iron levels (32). Similarly, in the present study, we determined by two-hybrid assays that the interaction of the full-length Grx4 with Fep1 was constitu-

tive and not modulated by iron. We found that both the TRX and the GRX domains of Grx4 interacted with Fep1. Surprisingly, we observed that the TRX domain of Grx4 interacted more strongly with Fep1 than with the GRX domain. Furthermore, the experiments revealed that the GRX domain interacted in an iron-dependent manner with the N-terminal region of Fep1. These results were different from those reported in the case of the *S. cerevisiae* monothiol glutaredoxins Grx3 and Grx4 with respect to their associations with Aft1 (38). In this case, two-hybrid experiments showed that each of the GRX and TRX domains of Grx3 and Grx4 interacted positively with Aft1, exhibiting similar levels of β-galactosidase activity, with no specification with respect to the interactions (between these polypeptides) as a function of iron availability. Although the nature of the difference between these respective observations is unclear, it is possible that the composition and length of the GRX and TRX domains may be contributing factors that would explain the differences between the results reported here and the results of other investigators (38). In this context, the GRX domains of *S. cerevisiae* Grx3 (residues 197 to 285) and Grx4 (residues 160 to 244) contain 88 and 84 amino acid residues, respectively, whereas the GRX domain (residues 105 to 244) of *S. pombe* Grx4 harbors 139 amino acid residues. Similarly, the TRX domains of *S. cerevisiae* Grx3 (residues 1 to 136) and Grx4 (residues 1 to 98) are shorter than the TRX domain of *S. pombe* Grx4 (residues 2 to 142). Alternatively, the differences between the respective results of the two-hybrid studies may be due to the fact that Fep1 (*S. pombe*) and Aft1 (*S. cerevisiae*) do not share significant amino acid sequence identity (only 15.2%). It is possible that these two proteins use distinct mechanisms or partners in their interactions with monothiol glutaredoxins.

When iron is abundant, Fep1 binds to DNA and forms a complex with Tup11 and probably Tup12, and the complexes act as corepressors to inhibit gene expression (51). We have previously shown that a minimal domain encompassing amino acid residues 405 to 541 of Fep1 is necessary for interaction with Tup11 (51). In the present study, deletion mapping experiments of the VP16-^{2}Fep1^{564} fusion protein showed that the C-terminal amino acid residues 405 to 501 are required for the interaction of Fep1 with the Grx4 protein. This minimal C-terminal region failed to interact with Tup11 (data not shown). Interestingly, this minimal module contains leucine-proline dipeptide repeats that have been suggested to play a role in protein-protein interactions (33). One of these repeats, ^{414}Leu-Pro-Pro-Ile-Leu-Pro^{419}, is also found in other iron-responsive transcriptional repressors, including SreA from *Aspergillus nidulans* (8), SreA from *Aspergillus fumigatus* (43) and SreP from *Penicillium chrysogenum* (7). Consistently, removal of amino acid residues 405 to 431 (in which the ^{414}Leu-Pro-Pro-Ile-Leu-Pro^{419} is located) abolished the association between the LexA-Grx4 and the VP16-^{432}Fep1^{564} fusion proteins (Fig. 5). However, the precise contribution of the ^{414}Leu-Pro-Pro-Ile-Leu-Pro^{419} motif, or of other residues located in the region encompassing amino acid residues 405 to 431 of Fep1, to the interaction between Fep1 and Grx4 must await a fine mapping of this minimal region. The region on Grx4 that is required for interaction with amino acid residues 405 to 501 of Fep1 is the TRX domain. This finding represents a novel function for this domain which is required for establishing a strong and iron-independent association with Fep1. A recent study (39) has shown that the TRX domains of both Grx3 and Grx4 of *S. cerevisiae* participate in the regulation of the actin cytoskeleton. However, whether their contribution to the repolarization of the actin cytoskeleton involves protein-protein interactions has not yet been ascertained. The TRX domain has also been proposed to be required for the targeting of the monothiol glutaredoxin Grx3 to the nucleus in *S. cerevisiae* (30). When the TRX and GRX domains of *S. pombe* Grx4 were separately tagged with GFP, cells expressing the TRX-GFP allele exhibited a pan-cellular fluorescence signal, with a large proportion being located to the nucleus (Fig. 9A). On the other hand, analysis by fluorescence microscopy showed that cells harboring the GRX domain fused to GFP appeared to have significantly less nuclear accumulation of fluorescence compared to that of the TRX-GFP fusion protein. However, presumably due to its small size (~42 kDa), the GRX-GFP still diffused across the nuclear envelope since its expression was sufficient to cause a slight derepression of the *fio1*$^{+}$ gene when the cells were grown under low-iron conditions (Fig. 8). As previously reported (30), our results also suggested that the TRX domain may significantly contribute to monothiol glutaredoxin Grx4 nuclear localization.

A second iron-responsive factor, denoted Php4, is critical for repressing the expression of the genes encoding iron-using proteins when iron levels are low in *S. pombe* (27, 28). Php4 is a subunit of the CCAAT-binding protein complex. In response to iron deficiency, Php4 is synthesized and interacts with the Php2/Php3/Php5 heterotrimer to mediate gene repression. When iron levels are high, Php4 is inhibited. *grx4*Δ mutant cells show a marked decrease in the transcription of the genes encoding iron-using proteins as a result of the presence of the constitutively active Php4. Under iron-replete conditions, Grx4 exerts an iron-dependent inhibitory effect on Php4 function, leading to Php4 inactivation. Grx4-mediated inactivation of Php4 involves an association between Grx4 and the C-terminal region of Php4 that encompasses amino acid residues 152 to 254 (26). Although the iron-dependent mechanism by which Grx4 inactivates Php4 function remains unclear, we determined that in cells undergoing a transition from low to high iron, Php4 (presumably with its partners) is exported from the nucleus to the cytoplasm by the exportin Crm1. Based on our studies, *S. pombe* represents an interesting model with which to investigate the iron-mediated signaling to iron regulators as the monothiol glutaredoxin Grx4 serves as a regulatory binding partner for both Fep1 and Php4 under conditions of low and high concentrations of iron, respectively.

The results show that Grx4 is required for the inhibition of Fep1 function in response to iron deficiency. How might this occur? Using coimmunoprecipitation experiments and two-hybrid analyses, we showed that Grx4 interacts with the C-terminal portion of Fep1 via its TRX domain. The association between the TRX domain and Fep1 was very strong and unmodified by cellular iron status. Under conditions of iron starvation, the GRX domain of Grx4 associated with Fep1 through its N terminus. This association between Grx4 and Fep1 would induce an inhibitory conformational change that inactivates the Fep1 DNA binding domain, blocking its interaction with chromatin and subsequently preventing its repressive effect on target gene expression. Conversely, under conditions of iron

excess, the GRX domain dissociates from the N-terminal portion of Fep1, resulting in the ability of Fep1 to bind to chromatin and thereby repressing the transcription of the target genes. Given the fact that it has been shown that Fep1 and monothiol glutaredoxin can form homodimers (13, 24, 36), one could propose that, under iron-limiting conditions, a dimer of Fep1 may associate with two GRX domains of Grx4, generating two Fep1 molecules clasps with two Grx4 molecules. In contrast, under iron-replete conditions, the two GRX domains of Grx4 would coordinate by themselves an iron-sulfur cluster, instigating conformational changes that would make the N terminus of Fep1 free and available for high-affinity DNA binding. Clearly, further studies will be needed to understand the reason why iron starvation-dependent inactivation of Fep1 function requires a monothiol glutaredoxin, a molecular determinant which is usually known to inactivate metalloregulators in response to high iron levels, not under low-iron-supply conditions.

ACKNOWLEDGMENTS

We are grateful to Gilles Dupuis and William Home for critically reading the manuscript and for their valuable comments. We thank Jude Beaudoin for help with preliminary experiments and stimulating discussions. We are thankful to Richard Rachubinski for the pmRFP-SKL plasmid encoding the red fluorescent protein.

M.J. and A.M. were recipients of studentships from the Fonds Québecois de la Recherche sur la Nature et les Technologies and the Fonds de la Recherche en Santé du Québec, respectively. This work was supported by the Natural Sciences and Engineering Research Council of Canada (NSERC) Grant MOP-238238-2010 to S.L. S.L. is supported by a Senior scholarship from the Fonds de la Recherche en Santé du Québec.

REFERENCES

1. **Beaudoin, J., J. Laliberté, and S. Labbé.** 2006. Functional dissection of Ctr4 and Ctr5 amino-terminal regions reveals motifs with redundant roles in copper transport. Microbiology **152:**209–222.
2. **Chao, L. Y., M. A. Marletta, and J. Rine.** 2008. Sre1, an iron-modulated GATA DNA-binding protein of iron-uptake genes in the fungal pathogen *Histoplasma capsulatum*. Biochemistry **47:**7274–7283.
3. **Chen, D., et al.** 2003. Global transcriptional responses of fission yeast to environmental stress. Mol. Biol. Cell **14:**214–229.
4. **Chen, O. S., et al.** 2004. Transcription of the yeast iron regulon does not respond directly to iron but rather to iron-sulfur cluster biosynthesis. J. Biol. Chem. **279:**29513–29518.
5. **Chung, W. H., K. D. Kim, Y. J. Cho, and J. H. Roe.** 2004. Differential expression and role of two dithiol glutaredoxins Grx1 and Grx2 in *Schizosaccharomyces pombe*. Biochem. Biophys. Res. Commun. **321:**922–929.
6. **Chung, W. H., K. D. Kim, and J. H. Roe.** 2005. Localization and function of three monothiol glutaredoxins in *Schizosaccharomyces pombe*. Biochem. Biophys. Res. Commun. **330:**604–610.
7. **Haas, H., K. Angermayr, and G. Stoffler.** 1997. Molecular analysis of a *Penicillium chrysogenum* GATA factor encoding gene (*sreP*) exhibiting significant homology to the *Ustilago maydis urbs1* gene. Gene **184:**33–37.
8. **Haas, H., I. Zadra, G. Stoffler, and K. Angermayr.** 1999. The *Aspergillus nidulans* GATA factor SREA is involved in regulation of siderophore biosynthesis and control of iron uptake. J. Biol. Chem. **274:**4613–4619.
9. **Halliwell, B., and J. M. Gutteridge.** 1992. Biologically relevant metal ion-dependent hydroxyl radical generation. FEBS Lett. **307:**108–112.
10. **Hentze, M. W., M. U. Muckenthaler, B. Galy, and C. Camaschella.** 2010. Two to tango: regulation of mammalian iron metabolism. Cell **142:**24–38.
11. **Herrero, E., and M. A. de la Torre-Ruiz.** 2007. Monothiol glutaredoxins: a common domain for multiple functions. Cell. Mol. Life Sci. **64:**1518–1530.
12. **Ho, S. N., H. D. Hunt, R. M. Horton, J. K. Pullen, and L. R. Pease.** 1989. Site-directed mutagenesis by overlap extension using the polymerase chain reaction. Gene **77:**51–59.
13. **Iwema, T., et al.** 2009. Structural basis for delivery of the intact $[Fe_2S_2]$ cluster by monothiol glutaredoxin. Biochemistry **48:**6041–6043.
14. **Jbel, M., A. Mercier, B. Pelletier, J. Beaudoin, and S. Labbé.** 2009. Iron activates *in vivo* DNA binding of *Schizosaccharomyces pombe* transcription factor Fep1 through its amino-terminal region. Eukaryot. Cell **8:**649–664.
15. **Kaplan, C. D., and J. Kaplan.** 2009. Iron Acquisition and transcriptional regulation. Chem. Rev. **109:**4536–4552.
16. **Keeney, J. B., and J. D. Boeke.** 1994. Efficient targeted integration at *leu1-32* and *ura4-294* in *Schizosaccharomyces pombe*. Genetics **136:**849–856.
17. **Kim, H. G., B. C. Kim, E. H. Park, and C. J. Lim.** 2005. Stress-dependent regulation of a monothiol glutaredoxin gene from *Schizosaccharomyces pombe*. Can. J. Microbiol. **51:**613–620.
18. **Kim, J., and J. P. Hirsch.** 1998. A nucleolar protein that affects mating efficiency in *Saccharomyces cerevisiae* by altering the morphological response to pheromone. Genetics **149:**795–805.
19. **Komarnitsky, P., E. J. Cho, and S. Buratowski.** 2000. Different phosphorylated forms of RNA polymerase II and associated mRNA processing factors during transcription. Genes Dev. **14:**2452–2460.
20. **Kumanovics, A., et al.** 2008. Identification of *FRA1* and *FRA2* as genes involved in regulating the yeast iron regulon in response to decreased mitochondrial iron-sulfur cluster synthesis. J. Biol. Chem. **283:**10276–10286.
21. **Labbé, S., B. Pelletier, and A. Mercier.** 2007. Iron homeostasis in the fission yeast *Schizosaccharomyces pombe*. Biometals **20:**523–537.
22. **Labbé, S., Z. Zhu, and D. J. Thiele.** 1997. Copper-specific transcriptional repression of yeast genes encoding critical components in the copper transport pathway. J. Biol. Chem. **272:**15951–15958.
23. **Li, H., et al.** 2011. Histidine 103 in Fra2 is an iron-sulfur cluster ligand in the [2Fe-2S] Fra2-Grx3 complex and is required for *in vivo* iron signaling in yeast. J. Biol. Chem. **286:**867–876.
24. **Li, H., et al.** 2009. The yeast iron regulatory proteins Grx3/4 and Fra2 form heterodimeric complexes containing a [2Fe-2S] cluster with cysteinyl and histidyl ligation. Biochemistry **48:**9569–9581.
25. **McNabb, D. S., K. A. Tseng, and L. Guarente.** 1997. The *Saccharomyces cerevisiae* Hap5p homolog from fission yeast reveals two conserved domains that are essential for assembly of heterotetrameric CCAAT-binding factor. Mol. Cell. Biol. **17:**7008–7018.
26. **Mercier, A., and S. Labbé.** 2009. Both Php4 function and subcellular localization are regulated by iron via a multistep mechanism involving the glutaredoxin Grx4 and the exportin Crm1. J. Biol. Chem. **284:**20249–20262.
27. **Mercier, A., B. Pelletier, and S. Labbé.** 2006. A transcription factor cascade involving Fep1 and the CCAAT-binding factor Php4 regulates gene expression in response to iron deficiency in the fission yeast *Schizosaccharomyces pombe*. Eukaryot. Cell **5:**1866–1881.
28. **Mercier, A., S. Watt, J. Bähler, and S. Labbé.** 2008. Key function for the CCAAT-binding factor Php4 to regulate gene expression in response to iron deficiency in fission yeast. Eukaryot. Cell **7:**493–508.
29. **Miller, J. H.** 1972. Experiments in molecular genetics. Cold Spring Harbor Laboratory Press, Cold Spring Harbor, NY.
30. **Molina, M. M., G. Belli, M. A. de la Torre, M. T. Rodriguez-Manzaneque, and E. Herrero.** 2004. Nuclear monothiol glutaredoxins of *Saccharomyces cerevisiae* can function as mitochondrial glutaredoxins. J. Biol. Chem. **279:**51923–51930.
31. **Muhlenhoff, U., et al.** 2010. Cytosolic monothiol glutaredoxins function in intracellular iron sensing and trafficking via their bound iron-sulfur cluster. Cell. Metab. **12:**373–385.
32. **Ojeda, L., et al.** 2006. Role of glutaredoxin-3 and glutaredoxin-4 in the iron regulation of the Aft1 transcriptional activator in *Saccharomyces cerevisiae*. J. Biol. Chem. **281:**17661–17669.
33. **Ostling, J., M. Carlberg, and H. Ronne.** 1996. Functional domains in the Mig1 repressor. Mol. Cell. Biol. **16:**753–761.
34. **Pelletier, B., J. Beaudoin, Y. Mukai, and S. Labbé.** 2002. Fep1, an iron sensor regulating iron transporter gene expression in *Schizosaccharomyces pombe*. J. Biol. Chem. **277:**22950–22958.
35. **Pelletier, B., J. Beaudoin, C. C. Philpott, and S. Labbé.** 2003. Fep1 represses expression of the fission yeast *Schizosaccharomyces pombe* siderophore-iron transport system. Nucleic Acids Res. **31:**4332–4344.
36. **Pelletier, B., A. Trott, K. A. Morano, and S. Labbé.** 2005. Functional characterization of the iron-regulatory transcription factor Fep1 from *Schizosaccharomyces pombe*. J. Biol. Chem. **280:**25146–25161.
37. **Pouliot, B., M. Jbel, A. Mercier, and S. Labbé.** 2010. *abc3+* encodes an iron-regulated vacuolar ABC-type transporter in *Schizosaccharomyces pombe*. Eukaryot. Cell **9:**59–73.
38. **Pujol-Carrion, N., G. Belli, E. Herrero, A. Nogues, and M. A. de la Torre-Ruiz.** 2006. Glutaredoxins Grx3 and Grx4 regulate nuclear localisation of Aft1 and the oxidative stress response in *Saccharomyces cerevisiae*. J. Cell Sci. **119:**4554–4564.
39. **Pujol-Carrion, N., and M. A. de la Torre-Ruiz.** 2010. Glutaredoxins Grx4 and Grx3 of *Saccharomyces cerevisiae* play a role in actin dynamics through their Trx domains, which contributes to oxidative stress resistance. Appl. Environ. Microbiol. **76:**7826–7835.
40. **Rodriguez-Manzaneque, M. T., J. Tamarit, G. Belli, J. Ros, and E. Herrero.** 2002. Grx5 is a mitochondrial glutaredoxin required for the activity of iron/sulfur enzymes. Mol. Biol. Cell **13:**1109–1121.
41. **Rouhier, N., J. Couturier, M. K. Johnson, and J. P. Jacquot.** 2010. Glutaredoxins: roles in iron homeostasis. Trends Biochem. Sci. **35:**43–52.
42. **Rutherford, J. C., et al.** 2005. Activation of the iron regulon by the yeast Aft1/Aft2 transcription factors depends on mitochondrial but not cytosolic iron-sulfur protein biogenesis. J. Biol. Chem. **280:**10135–10140.

43. **Schrettl, M., et al.** 2008. SreA-mediated iron regulation in *Aspergillus fumigatus*. Mol. Microbiol. **70:**27–43.
44. **Shakoury-Elizeh, M., et al.** 2010. Metabolic response to iron deficiency in *Saccharomyces cerevisiae*. J. Biol. Chem. **285:**14823–14833.
45. **Ueta, R., N. Fujiwara, K. Iwai, and Y. Yamaguchi-Iwai.** 2007. Mechanism underlying the iron-dependent nuclear export of the iron-responsive transcription factor Aft1p in *Saccharomyces cerevisiae*. Mol. Biol. Cell **18:**2980–2990.
46. **Ueta, R., A. Fukunaka, and Y. Yamaguchi-Iwai.** 2003. Pse1p mediates the nuclear import of the iron-responsive transcription factor Aft1p in *Saccharomyces cerevisiae*. J. Biol. Chem. **278:**50120–50127.
47. **Vojtek, A. B., J. A. Cooper, and S. M. Hollenberg.** 1997. Searching for interacting proteins with the two-hybrid system II, p. 29–42. *In* P. Bartel and S. Fields (ed.), The yeast two-hybrid system: a practical approach. Oxford University Press, New York, NY.
48. **Yamaguchi-Iwai, Y., A. Dancis, and R. D. Klausner.** 1995. AFT1: a mediator of iron regulated transcriptional control in *Saccharomyces cerevisiae*. EMBO J. **14:**1231–1239.
49. **Yamaguchi-Iwai, Y., R. Stearman, A. Dancis, and R. D. Klausner.** 1996. Iron-regulated DNA binding by the AFT1 protein controls the iron regulon in yeast. EMBO J. **15:**3377–3384.
50. **Yamaguchi-Iwai, Y., R. Ueta, A. Fukunaka, and R. Sasaki.** 2002. Subcellular localization of Aft1 transcription factor responds to iron status in *Saccharomyces cerevisiae*. J. Biol. Chem. **277:**18914–18918.
51. **Znaidi, S., B. Pelletier, Y. Mukai, and S. Labbé.** 2004. The *Schizosaccharomyces pombe* corepressor Tup11 interacts with the iron-responsive transcription factor Fep1. J. Biol. Chem. **279:**9462–9474.